

# Experimentally Estimating Phase Response Curves of Neurons: Theoretical and Practical Issues

Theoden Netoff<sup>1</sup>, Michael A Schwemmer<sup>2</sup>, and Timothy J Lewis<sup>2</sup>

1. Department of Biomedical Engineering, University of Minnesota, Minneapolis, MN 55455
2. Department of Mathematics, University of California, Davis, Davis, CA 95616

## 1. Introduction

A phase response curve (PRC) quantifies the response of a periodically firing neuron to an external stimulus (Figure 1). More specifically, it measures the phase shift of the oscillating neuron as a function of the phase that a stimulus is delivered. The task of generating a PRC for a real neuron seems straightforward: (1) If the neuron is not oscillating, then inject a constant current or apply a neuromodulator to make the neuron fire with the desired period; (2) Deliver a pulsatile stimulus at a particular phase in the neuron's periodic cycle, and measure the subsequent change in timing of the next spike (Figure 1 top panel); (3) Repeat these steps for many different phases (Figure 1 bottom panel). However, there are many subtle issues that complicate this seemingly simple process when dealing with real neurons.

Many of the complicating factors in generating PRCs arise from the fact that neurons are inherently noisy on several time-scales. There is usually a considerable amount of variation in the inter-spike intervals of "periodically" firing neurons. This jitter in inter-spike intervals confounds the change in phase that is due to a stimulus. Furthermore, neuronal firing is typically not stationary over the time-scales on which PRCs are measured, and a PRC can change significantly with the firing rate of a neuron. Other important issues that need consideration when constructing PRCs arise from the inherent nonlinearities and slow-time-scale processes of neuronal dynamics. These issues include determining the appropriate stimuli and deciding how long to wait between stimuli.

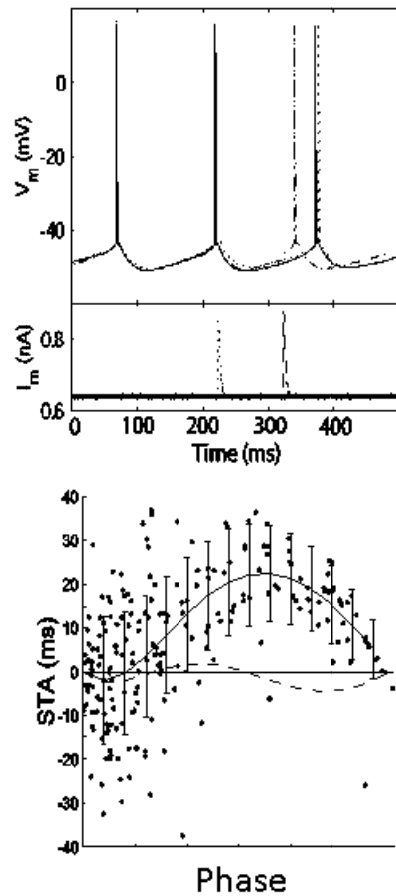


Figure 1. PRC measured from a cortical pyramidal neuron. Top panel: Voltage from an unperturbed periodically firing neuron (solid line); voltage from neuron stimulated with synaptic conductance near the end of the cycle, resulting in an advance of the spike from normal period (dash-dotted line); voltage from a neuron stimulated early in the cycle, resulting in slight delay of spike (dotted line). Bottom panel: Spike advance measured as a function of the phase of stimulation. Each dot represents the response to a stimulus. Solid line is a function fit to the raw data, estimating the PRC. Error bars indicate the standard deviation at each stimulus phase. The dashed line is the second order PRC, i.e. it indicates the effect of the synaptic input at that phase on the period following the stimulated period. Figure adapted from Netoff et al. 2005b.

In this chapter, we will discuss many of the complicating factors that arise when generating PRCs for real neurons or “realistic” model neurons. In sections 2 and 3, we focus on theoretical issues for which noise is not a factor. Section 2 addresses issues around the stimulus waveforms used to generate the PRC. Section 3 discusses the effects of slow-time-scale processes, such as spike frequency adaption, on the phase response properties of a neuron. In sections 4 and 5, we discuss issues that arise when measuring PRCs in “real-world” noisy conditions. Section 4 deals with issues that are present during data acquisition, and section 5 discusses fitting “noisy” PRC

data to extract the underlying PRC and quantifying the stochastic variation of the phase responses. Finally, in section 6, we describe an alternative method to generate PRCs using small amplitude white noise stimuli.

## 2. Choosing an appropriate stimulus

PRCs are often used to predict the phase-locking dynamics of coupled neurons, using either spike-time response curve (STRC) maps (e.g. (Canavier, 2005; Netoff et al., 2005) also see Chapter Z) or the theory of weakly coupled oscillators (e.g. (Ermentrout & Kopell, 1991; Kuramoto, 1984); also see Chapter X and Y) as follows:

(1) The STRC map approach can be used for networks in which synaptic inputs can be moderately strong but must be sufficiently brief. The limiting assumption of STRC map approach is that the effect of any input to a neuron must be complete before the next input arrives. In this case, the PRC can be used to predict the phase shift due to each synaptic input. Therefore, if one intends to use the STRC map method to predict phase-locking behavior, then PRCs should be generated using a stimulus that approximates the synaptic input in the neuronal circuit under study.

(2) The theory of weakly coupled oscillators can be used for completely general coupling but the total coupling current incident on a neuron at any time must be sufficiently small. The limiting assumption of this method is that the effects of the inputs sum linearly, i.e. the neurons respond to input like a time-dependent linear oscillator. The infinitesimal PRC (iPRC), which is used in the theory of weakly coupled oscillators, can be obtained from any PRC generated with sufficiently small perturbations (so long as the perturbation elicits a “measurable” response). Typically, current-based stimuli that approximate delta-functions are used.

As indicated above, the choice of stimulus used to generate a PRC depends on the intended use of the PRC. It also depends on the need for realistic stimuli and ease of implementation. In

this section, we will address some of the issues involved in choosing an appropriate stimulus waveform to generate a PRC. For the case of small amplitude stimuli, we will also describe the relationships between PRCs generated with different stimulus waveforms.

## 2.1 Stimulus waveforms

### 2.1.1 Current-based synaptic input:

Perhaps the simplest stimulus waveform used to measure a neuron's PRC is a square pulse of current. Square wave current stimuli are easy to implement in models and in a real neuron, using a waveform generator. A possible drawback is that square wave pulses do not resemble synaptic conductances (however, see section 2.2) .

A current stimulus waveform that has a shape similar to realistic synaptic input is an alpha function

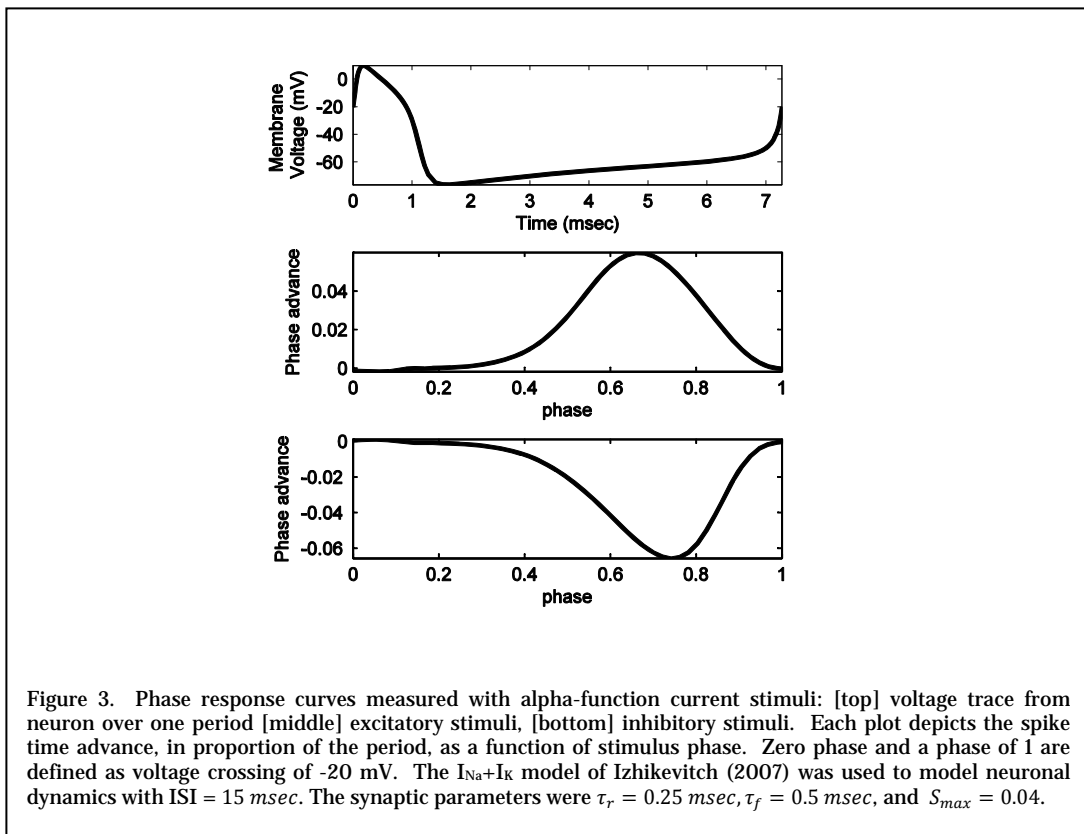
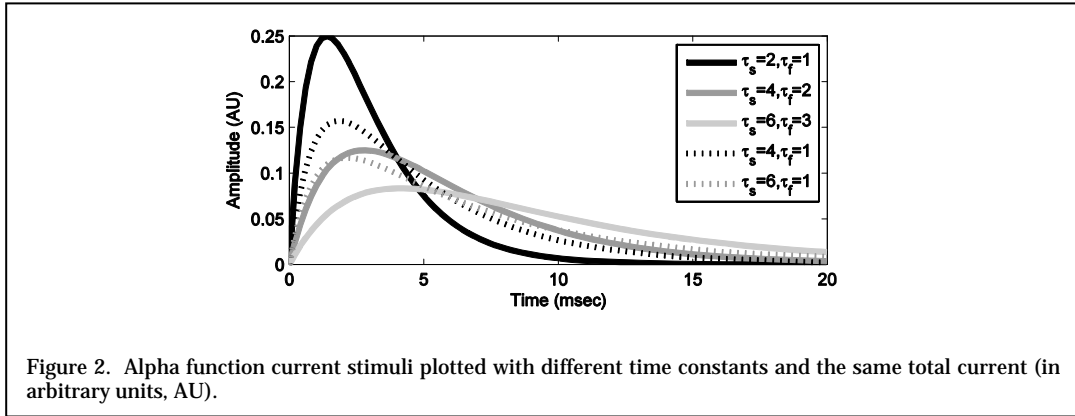
$$I_{syn}(t) = S_{max} \frac{1}{\tau_f - \tau_r} \left( e^{-\frac{t}{\tau_f}} - e^{-\frac{t}{\tau_r}} \right), \quad t \geq 0,$$

where  $S_{max}$  controls the amplitude of the synaptic current,  $\tau_f$  is the time constant that controls the decay ("fall") of the synaptic current, and  $\tau_r$  is the time constant that controls the rise time of the synaptic current. Here,  $t = 0$  is the time at the onset of each synaptic input. Examples of alpha functions with different coefficients are plotted in Figure 2. The coefficients of the alpha function current stimulus can be chosen in order to fit the post-synaptic potentials (PSPs) measured in neurons of interest.<sup>1</sup> In the neocortex, physiologically reasonable values for the synaptic conductance time constants are  $\tau_f \approx 1.8$  msec and  $\tau_r \approx 1.4$  msec for fast excitatory synapses and  $\tau_f \approx 3.5$  msec and  $\tau_r \approx 1.0$  msec for fast inhibitory synapses (Cruikshank, Lewis, & Connors, 2007). The peak amplitude is synapse-specific and depends on the resistance of the neuron. We usually adjust the amplitude of the synaptic current so that it elicits a PSP of ~1 mV

---

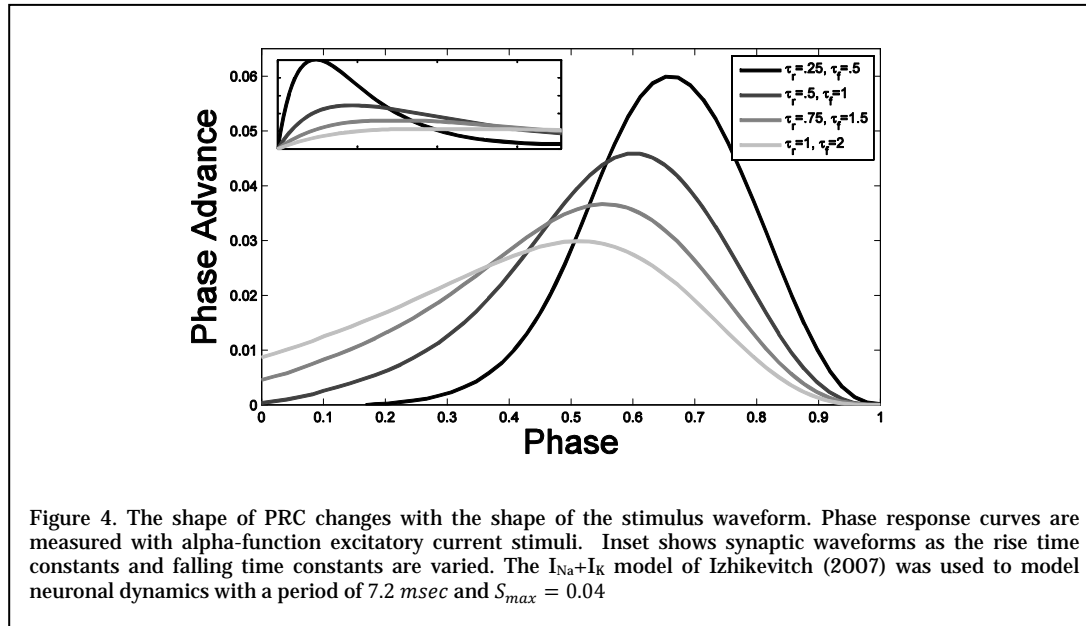
<sup>1</sup> The time constants of the synaptic currents will be faster than those for the PSP because the current waveform is filtered due to the RC properties neuronal membrane. To find the time constants of the synaptic currents, one can adjust these time constants until the current stimulus induces a PSP waveform that adequately matches an actual PSP.

in amplitude. Figure 3 shows PRCs generated using an alpha function current stimulus with a positive  $S_{max}$  to simulate an excitatory synaptic input (top) and a negative  $S_{max}$  to simulate an inhibitory synapse (bottom).



The shape of the PRC can be significantly affected by the shape of the stimulus waveform used to generate it. PRCs measured from the same neuron using excitatory currents with different time constants are shown in Figure 4. As the synaptic time constants increase, the PRC

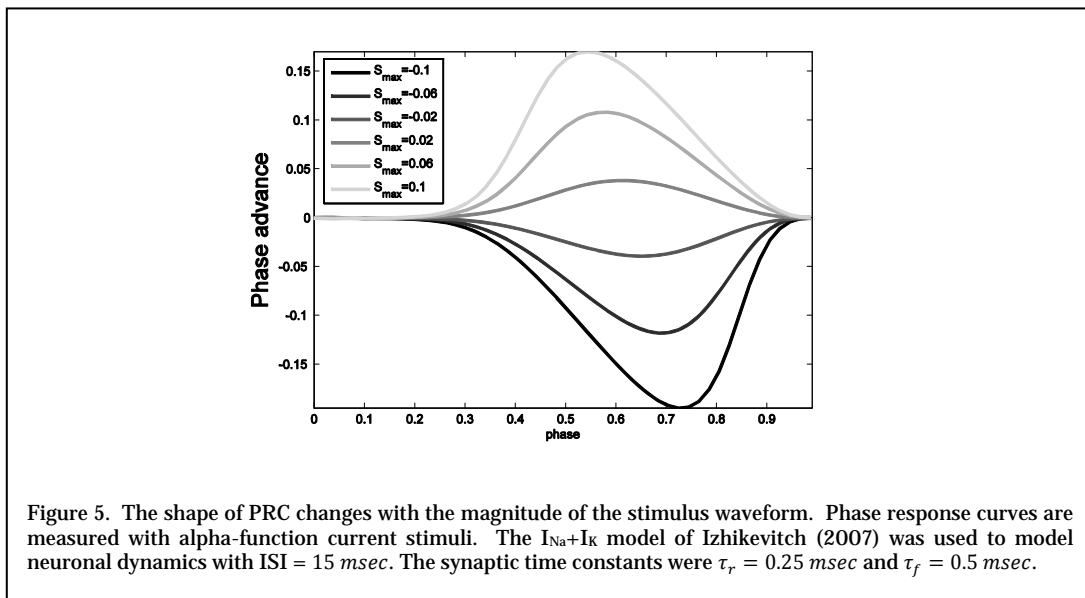
peak shifts down and to the left. This shift in the PRC is associated with changes in phase-locking of synaptically coupled neurons; simply by slowing the time constants of the synapses, it is possible for a network to transition from synchronous firing to asynchronous firing (Lewis & Rinzel, 2003; Netoff et al., 2005; Van Vreeswijk, Abbott, & Ermentrout, 1994).



The PRC can also be affected by the magnitude of the stimulus used to generate it. As shown in the example in Figure 5, the peak of the PRC typically shifts up and to the left as the magnitude of excitatory input increases. PRCs for inhibitory pulses are generally flipped compared to those for excitatory pulses, and the peak in the PRC typically shifts down and to the right as the magnitude of inhibitory input increases. For sufficiently small input, the magnitude of the PRC scales approximately linearly with the magnitude of the input. In fact, for sufficiently small input, the changes in the PRC that occur due to changes in the stimulus waveform can be understood in terms of a convolution of the stimulating current with the neuron's so-called infinitesimal PRC. This will be described more fully in section 2.2. Some of the changes in the PRC that occur in response to changes of the stimuli with large magnitudes follow the same trends found for small stimuli, however other changes are more complicated and involve the nonlinear properties of neurons.

When stimulating a neuron, the maximum a neuron's spike can be advanced is to the time of the stimulus. In other words, the spike cannot be advanced to a time before the stimulus was applied. Therefore, the spike advance is limited by causality. Often we plot the causality limit along with the PRC to show the maximal advance (as shown in Figure 16). When plotting PRC's measured from neurons if the stimulus was too strong much of the data will hug the causality limit for a significant portion of the phase,. This indicates that the stimulus is eliciting an action potential at these phases. If this is the case, we will drop the stimulus strength down. Because each neuron we record has a different resistance, it is not possible to choose one stimulus amplitude that works for every cell. We often have to adjust the amplitude. If the stimulus amplitude is too weak, we find the PRC is indistinguishable from flat.

The line of causality can affect the estimate of the PRC as well. If the neuron is close to the line of causality, it effectively truncates the noise around the PRC. PRC's measured using excitatory synaptic inputs are affected more by the line of causality than those measured with inhibitory synaptic inputs, where the effect is to generally delay the next spike. In another chapter in this book, it will be addressed how the truncation of the noise can affect the estimation of the PRC and how to correct for it.



### 2.1.2 Conductance-based synaptic input:

When a neurotransmitter is released by a presynaptic cell, it opens ion channels in the postsynaptic cell, evoking a synaptic current carried by the flow of ions through the cell membrane. The synaptic current depends on number of channels opened (i.e. the activated synaptic *conductance*) and the potential across the membrane. To simulate a more realistic “conductance-based” synapse, an alpha function can be used to describe the synaptic conductance waveform which is then multiplied by synaptic driving force (the difference between the membrane potential  $V$  and the reversal potential of the synaptic current  $E_{syn}$ ) to calculate the synaptic current

$$I_{syn}(t) = G_{syn}(t) (E_{syn} - V(t)), \quad t \geq 0,$$

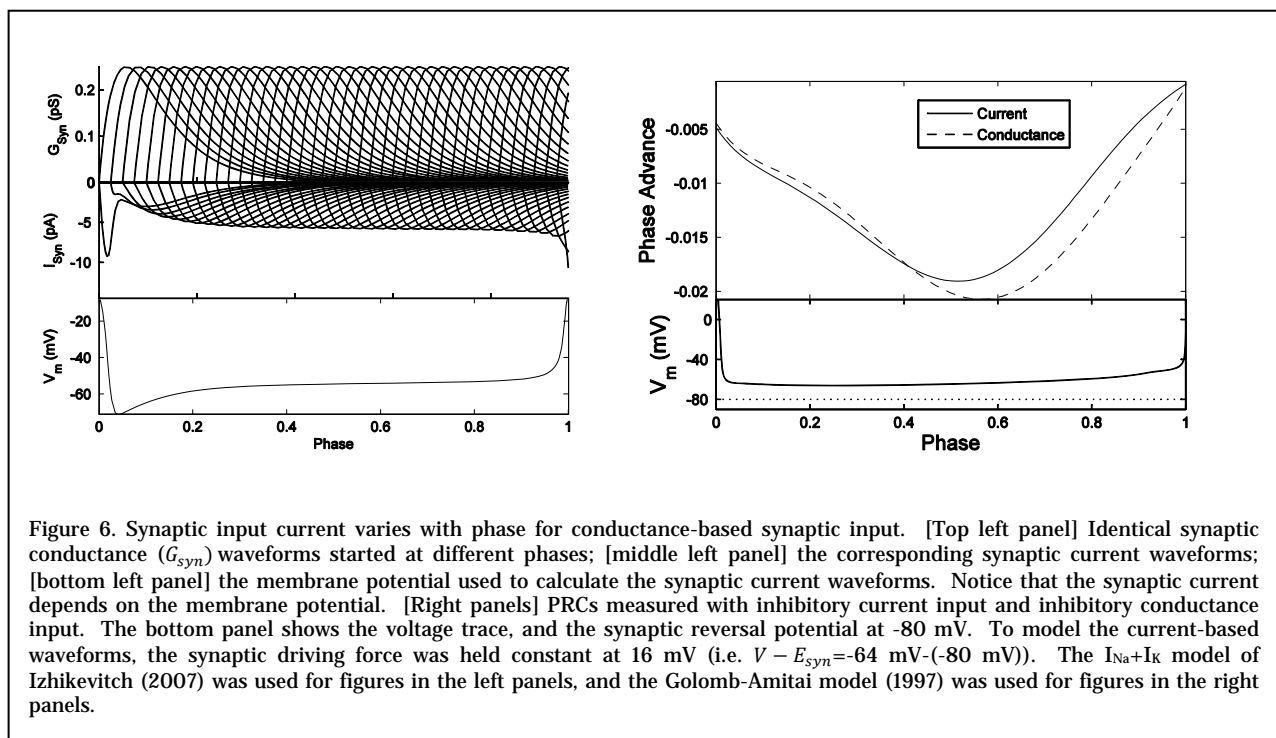
where the synaptic conductance waveform  $G_{syn}(t)$  is defined to be

$$G_{syn}(t) = g_{syn} \frac{1}{\tau_s - \tau_f} \left( e^{-\frac{t}{\tau_s}} - e^{-\frac{t}{\tau_f}} \right), \quad t \geq 0.$$

The parameter  $g_{syn}$  scales the amplitude of the synaptic conductance. Note that stimulating a neuron with a conductance waveform requires a closed loop feedback system, called a dynamic clamp. The details of a dynamic clamp will be discussed section 4.1.

The synaptic reversal potential is calculated using the Nernst equation if the channels only pass one ion, or the Goldman-Hodgkin-Katz equation if it passes multiple ions (Hille, 1992). Excitatory glutamatergic ion channels are cationic, passing some sodium and potassium ions, and therefore the associated excitatory synaptic current reversal potential is usually set near 0 mV. Inhibitory GABAergic ion channels pass mainly chloride or potassium ions, and therefore the associated inhibitory synaptic reversal potential is usually set near -80 mV. The time constants for synaptic conductances are very similar to those previously quoted for synaptic currents.

In Figure 6, the synaptic conductance profiles and corresponding current waveforms for an excitatory synaptic conductance-based input are plotted for different input phases, as illustrated in the Golomb-Amitai model neuron (Golomb & Amitai, 1997). As the neuron's membrane potential changes over the cycle so does the synaptic driving force. Thus, the synaptic current waveform will be different for different input phases. For this reason, a PRC measured with a conductance-based input will be different from a PRC measured using a stimulus with a fixed current waveform. For excitatory conductance-based synaptic inputs, the input current can even reverse direction when the action potential passes through the excitatory synaptic reversal potential. Differences between PRC generated with inhibitory conductance-based input current-based input are more pronounced than for excitatory input because the cell's voltage between action potentials is much closer to the inhibitory reversal potential than for the excitatory reversal potential. This results in larger fractional changes of the driving force (and therefore input current) when compared to excitatory synapses.



## 2.2 The infinitesimal phase response curve (iPRC)

The infinitesimal phase response curve (iPRC or  $Z$ ) is a special PRC that directly measures the sensitivity of a neuronal oscillator to small input current<sup>2</sup> at any given phase. The iPRC is used in the theory of weakly coupled oscillators to predict the phase-locking patterns of neuronal oscillators in response to external input or due to network connectivity (Ermentrout & Kopell, 1991; Kuramoto, 1984) see also Chapters X and Y). For mathematical models, the iPRC can be computed by linearizing the system about the stable limit cycle and solving the corresponding adjoint equations ((Ermentrout & Chow, 2002), see also Chapter X). Equivalently, the iPRC can be constructed by simply generating a PRC in a standard fashion using a small delta-function<sup>3</sup> current pulse and then normalizing the phase-shifts by the net charge of the pulse (the area of the delta-function). More practically, the iPRC can be obtained using any stimulus that approximates a delta-function, i.e. any current stimulus that is sufficiently small and brief. Typically, small brief square pulses are used. Note that, for sufficiently small stimuli, the system will behave like a time-dependent linear oscillator, and therefore the iPRC is independent of the net charge of the stimulus that was used. When generating approximations of a real neuron's iPRC, it is useful to generate iPRCs for at least two amplitudes to test for linearity and determine if a sufficiently small stimulus was used.

### 2.2.1 Relationship between general PRCs and the iPRC

The iPRC measures the *linear* response of an oscillating neuron (in terms of phase shifts) to small delta-function current pulses. Therefore, it can serve as the impulse response function for the oscillatory system: The phase-shift due to a stimulus of arbitrary waveform with sufficiently small amplitude can be obtained by computing the integral of the stimulus weighted by the

---

<sup>2</sup> In general, the iPRC is equivalent to the gradient of phase with respect to all state variables evaluated at all points along the limit cycle (i.e. it is a vector measuring the sensitivity to perturbations in any variable). However, because neurons are typically only perturbed by currents, the iPRC for neurons is usually taken to be the voltage component of this gradient ( $\frac{\partial \phi}{\partial v}$ ) evaluated along the limit cycle.

<sup>3</sup> A delta-function is a pulse with infinite height and zero width with an area of one. Injecting a delta-function current into a cell corresponds to instantaneously injecting a fixed charge into the cell, which results in an instantaneous jump in the cell's membrane potential by a fixed amount.

iPRC. Thus, a PRC of a neuron for any particular current stimulus can be estimated from the “convolution”<sup>4</sup> of the stimulus waveform and the neuron’s iPRC

$$PRC(\phi) \cong \int_0^{\infty} Z(t + \phi T) I_{stim}(t) dt, \quad (1)$$

where  $PRC(\phi)$  is the phase shift in response of a neuron with an iPRC  $Z(t)$  and a current stimulus of waveform  $I_{stim}(t)$ , and  $\phi$  is the phase of the neuron at the onset of the stimulus. Note that equation 1 assumes that the relative phase of the neuron  $\phi$  is a constant over the entire integral. However, because only small stimuli are considered, phase shifts will be small, and thus this assumption is reasonable.

### 2.2.2 Calculating PRCs from iPRCs

Assuming that the functional forms of the stimulus (as chosen by the experimenter) and the iPRC (as fit to data) are known, an estimate of the PRC can be calculated using equation 1. From a practical standpoint, the interval of integration must be truncated so that the upper limit of the interval is  $t_{max} < \infty$ . By discretizing  $\phi$  and  $t$  so that  $t_j = j \Delta t$  and  $\phi_j = j \Delta t/T$  with  $j = 1 \dots N, \Delta t = t_{max}/N$ , equation becomes

$$PRC(\phi_j) \cong \sum_{k=0}^{N-1} Z(t_k + \phi_j T) I_{stim}(t_k) \Delta t \quad (2)$$

(Note that a simple left Reimann sum is used to approximate the integral, but high order numerical integration could be used for greater accuracy). Equation 2 can be used to directly compute an approximation of the PRC in the time-domain. In this direct calculation,  $t_{max}$  should be chosen sufficiently large to ensure that the effect of the stimulus is almost entirely accounted for. In the case of small pulsatile stimuli, one period of the neuron’s oscillation is usually sufficient (i. e.  $t_{max} = T$ ).

---

<sup>4</sup> The definition of a convolution is  $g * f(\psi) = \int g(\psi - t) f(t) dt = \int g(-(t - \psi)) f(t) dt$ , so technically,  $PRC(\phi) = Z * I(-\phi T)$ .

The PRC could also be calculated by solving equation 2 using discrete Fourier transforms (DFTs)

$$PRC(\phi_j) \cong \frac{1}{N} \sum_{n=0}^{N-1} \hat{Z}_n \hat{I}_{(N-1)-n} e^{-i2\pi n \phi_j T / t_{max}} \Delta t \quad (3)$$

where  $\hat{Z}_n$  and  $\hat{I}_n$  are coefficients of the  $n^{\text{th}}$  modes of the DFTs of the discretized  $Z$  and  $I_{stim}$ , as defined by

$$x(t_j) = \sum_{n=0}^{N-1} \hat{x}_n e^{\frac{i2\pi n t_j}{t_{max}}}, \quad \hat{x}_n = \frac{1}{N} \sum_{j=0}^{N-1} x(t_j) e^{-i2\pi n t_j / t_{max}} \quad (4)$$

Note that, because the DFT assumes that functions are  $t_{max}$ -periodic, a  $PRC(\phi_j)$  calculated with this method will actually correspond to phase shifts resulting from applying the stimulus  $I_{stim}$   $t_{max}$ -periodically. To minimize this confounding effect,  $t_{max}$  should be two or three times the intrinsic period of the neuron for small pulsatile stimuli (i. e.  $t_{max} = 2T$  or  $3T$ ).

### 2.2.3 Calculating iPRC from the PRC measured with current-based stimuli:

If a PRC was measured for a neuron using a stimulus that had a sufficiently small magnitude, then the iPRC of the neuron can be estimated by “deconvolving” the functional form of the PRC with the stimulus waveform, i.e. solving equation 2 for  $Z(t_j)$ . Deconvolution can be done in the time-domain or the frequency-domain. Equation 3 shows that the  $n^{\text{th}}$  mode of the DFTs of the discretized PRC is  $\widehat{PRC}_n = \hat{Z}_n \hat{I}_{(N-1)-n} \Delta t$ . Therefore, the iPRC can be computed by

$$Z(t_j) \cong \sum_{n=0}^{N-1} \left( \frac{\widehat{PRC}_n}{\hat{I}_{(N-1)-n} \Delta t} \right) e^{i2\pi n \phi_j T / t_{max}}. \quad (5)$$

We can also directly solve equation 2 for the iPRC,  $Z(t_j)$ , in the time domain by noting that

$$\begin{aligned}
PRC(\phi_j) &\cong \sum_{k=1}^N Z(t_k + \phi_j T) I_{stim}(t_k) \Delta t \\
&= \sum_{k=1}^N I_{stim}(t_k - \phi_j T) Z(t_k) \Delta t,
\end{aligned} \tag{6}$$

which can be written in matrix form as

$$\overline{PRC} \cong \overline{I}_{stim} \overline{Z}, \tag{7}$$

where  $\overline{PRC}$  and  $\overline{Z}$  are the vectors representing the discretized PRC and iPRC respectively, and  $\overline{I}_{stim}$  is an  $N \times N$  matrix with the  $j, k^{\text{th}}$  element  $I_{stim}(t_k - \phi_j T)$ . Therefore, we can find the iPRC  $\overline{Z}$  by solving this linear system. Note that this problem will be well-posed because all rows of  $\overline{I}_{stim}$  are shifts of the other rows.

A related method for measuring the iPRC using a white noise current stimulus will be discussed in section 6.

#### 2.2.4 iPRCs, PRCs and conductance-based stimuli

As inferred from section 2.1.2, the synaptic waveform for conductance-based stimuli is not phase invariant. However, the ideas in previous sections can readily be extended to incorporate conductance-based stimuli. The PRC measured with a synaptic conductance is related to the iPRC by

$$PRC(\phi) \cong \int_0^{\infty} Z(t + \phi T) g_{syn}(t) (E_{syn} - V(t + \phi T)) dt. \tag{8}$$

Assuming that the functional forms of the stimulus, the iPRC and the membrane potential are known, an estimate of the PRC for conductance-based stimuli can be calculated in a similar manner to that described for current-based stimuli in section 2.2.2. That is, the PRC can be computed in the time-domain or frequency domain, using

$$PRC(\phi_j) \cong \sum_{k=0}^{N-1} Z(t_k) \left[ g_{syn}(t_k - \phi_j T) (E_{syn} - V(t_k)) \right] \Delta t \quad (9)$$

$$= - \sum_{n=0}^{N-1} \hat{z}_n \hat{v}_n \hat{g}_{(N-1)-n} e^{-i2\pi n \phi_j T / t_{max}} \Delta t, \quad (10)$$

where  $\hat{v}_n$  and  $\hat{g}_n$  are the  $n^{\text{th}}$  modes of the DFTs of the discretized functions  $(V(t) - E_{syn})$  and  $g_{syn}(t)$ . Furthermore, the iPRC can be calculated from the PRC in the frequency-domain by noting that the  $n^{\text{th}}$  mode of the DFTs of the discretized PRC is  $\widehat{PRC}_n = -\hat{z}_n \hat{v}_n \hat{g}_{(N-1)-n} \Delta t$  for conductance-based stimuli (see equation 10), therefore

$$Z(t_j) = - \sum_{n=0}^{N-1} \left( \frac{\widehat{PRC}_{-n}}{\hat{v}_n \hat{g}_{(N-1)-n} \Delta t} \right) e^{i2\pi n \phi_j T / t_{max}}. \quad (11)$$

When computing the iPRC in the time-domain, we can first “deconvolve” equation 8 to find the product  $(E_{syn} - V(t)) Z(t)$ , and then divide out the driving force to find the  $Z(t)$ . Note that numerical error could be large when  $(E_{syn} - V(t_k))$  is small, therefore care should be taken at these points (e.g. these points could be discarded).

Estimates of the iPRCs for a real neuron that are calculated from PRCs measured with excitatory synaptic conductance in one case and inhibitory synaptic conductance in another are shown in Figure 7 (Netoff, Acker, Bettencourt, & White, 2005). While the measured PRCs look dramatically different, the iPRCs are quite similar, indicating that the main difference in the response can be attributed to changes in the synaptic reversal potential. The remaining differences between the estimated iPRCs are likely due to small changes in the state of the neuron, error introduced by fitting the PRCs, and/or the fact that the response of the neuron to the stimuli is not perfectly linear.

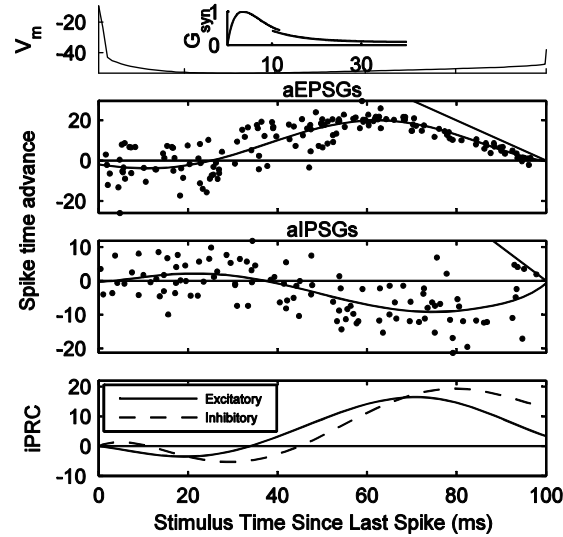


Figure 7. Estimates of the infinitesimal PRC (iPRC) for a pyramidal neuron from CA1 region of the hippocampus as calculated using PRCs. A synaptic conductance stimulus was used to generate PRCs of the neuron, and then the shape of the synaptic waveform was deconvolved from the PRC to estimate the iPRC. (Top panel) Voltage trace of neuron over one period. Inset is the synaptic conductance waveform. (Middle two panels) PRCs measured with excitatory conductances (upper) and inhibitory conductances (lower). (Bottom panel) iPRCs estimated using the excitatory and the inhibitory PRCs. The iPRCs from the two data sets, despite being measured with completely different waveforms, are similar. Figure modified from Netoff et al, 2005a

### 3. Dealing with slow-time-scale dynamics in neurons

Processes that act on relatively slow time scales can endow a neuron with the “memory” of stimuli beyond a single cycle. In fact, a stimulus applied to one cycle is never truly isolated from other inputs. In this section we will address how neuronal memory can affect the phase response properties of a neuron. Specifically, we will discuss how stimuli can affect the cycles following the cycle in which the neuron was stimulated and how to quantify these effects (Section 3.1). We also address how the effect of repeated inputs can accumulate over many periods, resulting in accommodation of the firing rate and alteration of the PRC (Section 3.2).

#### 3.1 Higher-order PRCs

A stimulus may not only affect the inter-spike intervals (ISIs) in which it is applied but may also affect the ISIs of the following cycles, although usually to a lesser degree. This can happen

in two ways. The first is when the stimulus starts in one cycle but continues into the next cycle. The second is through neuronal memory. For example, a phase shift of a spike during one cycle may result in compensatory changes in the following cycle, or the stimuli may significantly perturb a slow process such as an adaption conductance. Often a large spike advance is followed by a small delay in the next period (Netoff et al., 2005; Oprisan & Canavier, 2001). As mentioned earlier, the PRC represents the phase shifts of the *first* spike following the onset of the stimulus, so the PRC measured this way can be considered the “first order PRC”. The additional phase shifts of the second spike (or  $n^{\text{th}}$  spike) following the onset of the stimulus versus the phase of the stimulus onset is called the “second order PRC” (or  $n^{\text{th}}$  order PRC). Examples of first, second and third order PRCs are shown in Figure 8. The higher order PRCs are usually small as compared to the first order PRC, but can have significant implications in predicting network behavior when accounted for (Oprisan & Canavier, 2001).

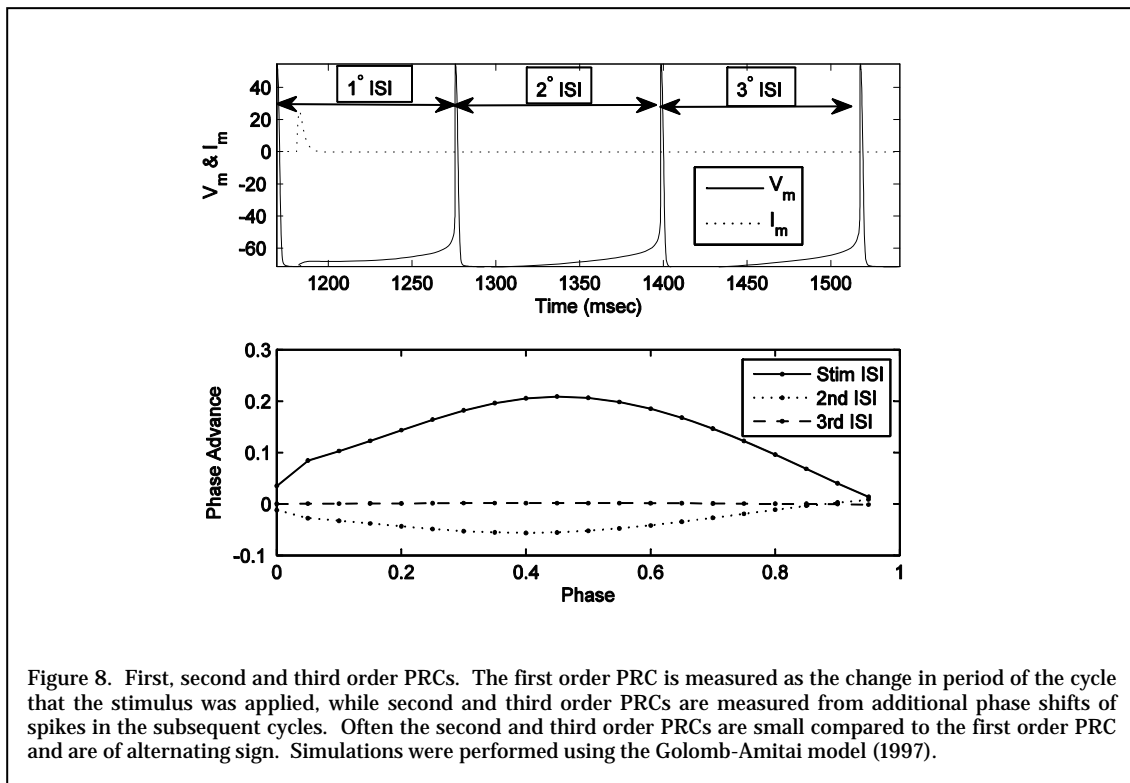


Figure 8. First, second and third order PRCs. The first order PRC is measured as the change in period of the cycle that the stimulus was applied, while second and third order PRCs are measured from additional phase shifts of spikes in the subsequent cycles. Often the second and third order PRCs are small compared to the first order PRC and are of alternating sign. Simulations were performed using the Golomb-Amitai model (1997).

### 3.2 Functional PRCs

Many neurons exhibit significant amount of accommodation when a repeated stimulus is applied. Thus, the shape of the PRC can depend on whether the perturbed cycle is measured before or after the accommodation. Usually, the PRC is measured by applying a single stimulus every few periods, in order to let the neuron recover from the stimulus and return to baseline firing rate. If the stimulus is repeated at each cycle and the same time lag, the neuron may accommodate to the synaptic input by changing the ISI over the first few cycles. One approach to deal with the accommodation is to measure the phase advance after the neuron has accommodated to the input and reached a steady-state response. The phase response curve from the accommodated neuron is termed the functional phase response curve (fPRC) (Cui, Canavier, & Butera, 2009). The method is illustrated in Figure 9. The PRC taken from the first stimulus interval looks different from the last train. Under conditions where a neuron may accommodate significantly during network dynamics, the predictions of network phase locking using the fPRC may produce more accurate results than predictions using standard PRCs.

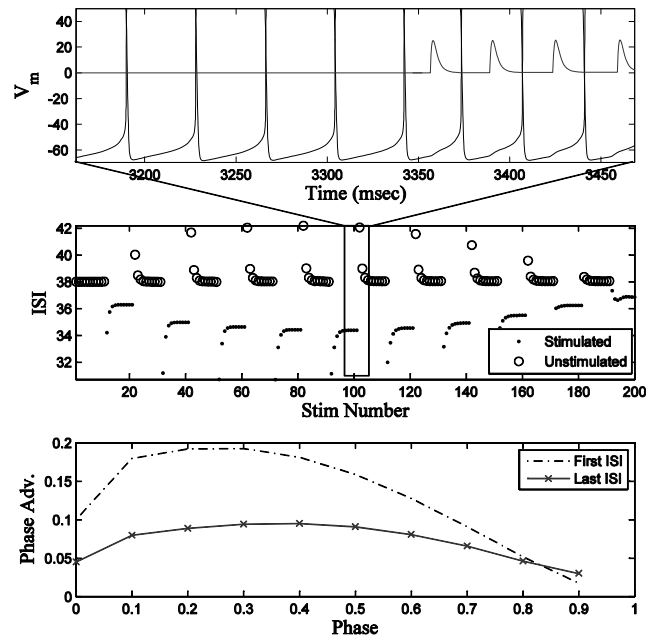


Figure 9. Functional PRC takes accommodation into consideration. The neuron is stimulated at the same phase for many cycles, and the PRC is determined from the average interspike intervals averaged over the last cycles. (Top trace) Voltage (in mV) and current for a stimulus applied repeatedly at a fixed phase. Time series taken from one set of stimuli shown in middle panel. (Middle) Interspike intervals (ISIs): circles represent unstimulated cycles; dots are stimulated periods. The phase of the stimulus is systematically varied from the earliest to latest across the stimulus trains. Simulations were performed using the Golomb-Amitai model (1997). (Bottom) PRCs without accommodation (calculated from first ISI) and with accommodation (calculated from last ISI).

## 4. Issues in PRC data acquisition

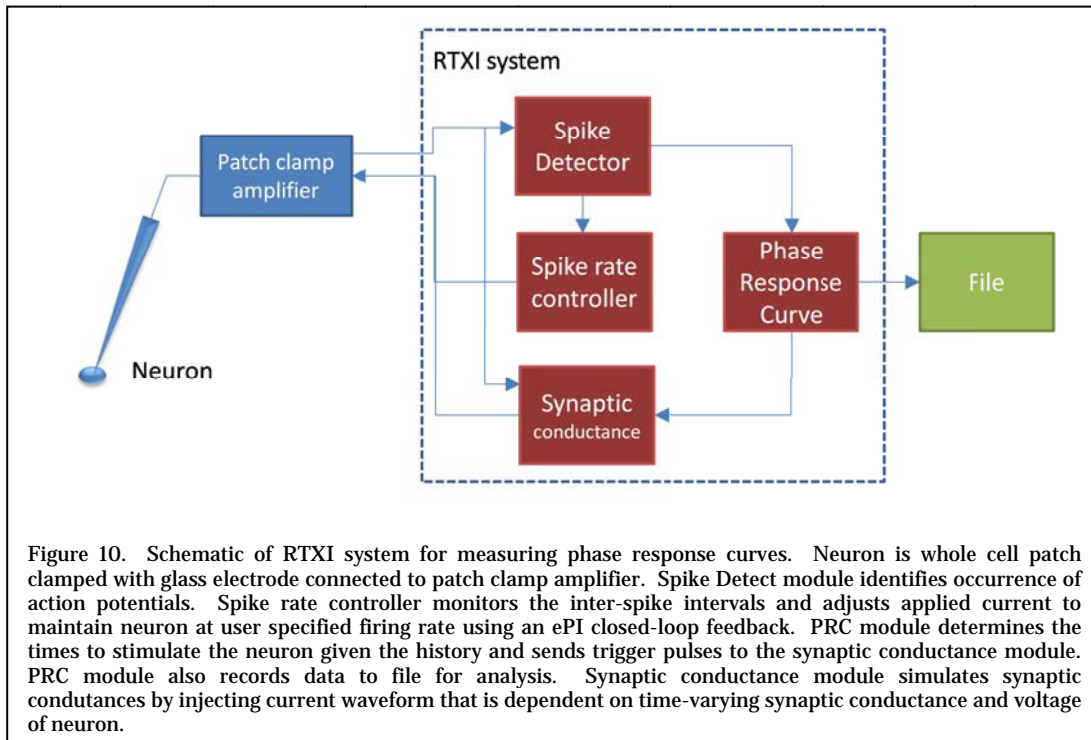
On the time-scale of a full PRC experiment, the neuron's firing rate can drift significantly. This drift can confound the small phase shifts resulting from the stimuli. "Closed-loop" experimental techniques can be used to counteract this drift and maintain a stable firing rate over the duration of the experiment. In this section 4.1, we introduce the dynamic clamp technique, which enables closed loop experiments (section 4.1), and we describe a method for using the dynamic clamp to control the spike rate in order to reduce firing rate drift over the duration of the experiment (section 4.2). We also show how the dynamic clamp can also be used

to choose the phases of stimulation in a quasi-random manner, which can minimize sampling bias (section 4.3).

#### **4.1 Open-loop and closed-loop estimation of the PRC**

Historically, patch clamp experiments have been done in open-loop, where a pre-determined stimulus is applied to the neuron and then the neuron's response is measured. With the advent of fast analog-to-digital sampling cards in desktop computers, it has been possible to design experiments that require real-time interactions between the stimulus and the neuron's dynamics in a closed-loop fashion, called a dynamic-clamp (Sharp, O'Neil, Abbott, & Marder, 1993).

There are many different real-time systems available for dynamic clamp experiments (Prinz, Abbott, & Marder, 2004). We use the Real-Time eXperimental Interface (RTXI) system (A. D. Dorval 2nd, Bettencourt, Netoff, & White, 2007; A. D. Dorval, Christini, & White, 2001; A. D. Dorval, Bettencourt, Netoff, & White, 2008), which is an open-source dynamic clamp based on real-time Linux. It is freely available to the public for download at <http://www.rtxi.org>. Modules for controlling the firing rate of the neuron, simulating synapses and measuring the PRC can be downloaded with the RTXI system. The RTXI system is modular, allowing one to write small modules that perform specific tasks and then connect them together to run full sets of experiments. Figure 10 illustrates the modules used to generate PRCs experimentally. We note that the modular design makes it relatively easy to replace a synaptic conductance module with a module to trigger a pico-spritzer to inject neurotransmitters proximal to the dendrite to simulate synapses.



## 4.2 Controlling spike rate

The PRC measures the neuron's deviation from the natural period due to a stimulus. If the firing rate of the neuron drifts over the time that PRC data is collected, then the measured spike advance caused by the synaptic perturbation will be confounded with the drift in the spike rate. An advantage of closed-loop measurements is that the baseline applied current can be adjusted slightly from cycle to cycle to maintain the firing rate close to a desired frequency.

To maintain the firing rate of the neuron, we developed an event based proportional-integral (ePI) controller (Miranda-Dominguez, Gonía, & Netoff, 2010). The baseline current is adjusted immediately after the detection of the spike and only small changes in current are allowed from cycle to cycle. The current at each spike is calculated as  $I(n) = K_p e(n) + K_i \sum_{j=0}^n e(j)$ , where  $e(n)$  is the difference between the measured inter-spike interval (ISI) on cycle  $n$  and the target period,  $K_p$  is the proportional constant, and  $K_i$  is an integration constant. It is possible to determine optimal values for these coefficients based on the gain of the neuron's

response to change in current and the time to settle, which is out of the scope of this chapter and will be published elsewhere. We have found that for most neurons using  $K_p = 6 \times 10^{-12}$  and  $K_i = 6 \times 10^{-10}$  works well. Figure 11 demonstrates the effects of the spike rate controller. The ISIs are plotted for an open-loop experiment in which a constant current is injected into a neuron and for a closed-loop experiment in which a current is adjusted to maintain the neuron at a desired firing rate. The mean ISI in the open-loop experiments undergoes a drift of ~10-20 msec, whereas the mean ISI in the closed-loop experiments stays very close target period of 100 msec. The autocorrelation is also shown to show that the method does not introduce any significant correlation, which occurs if the feedback loop begins to oscillate.

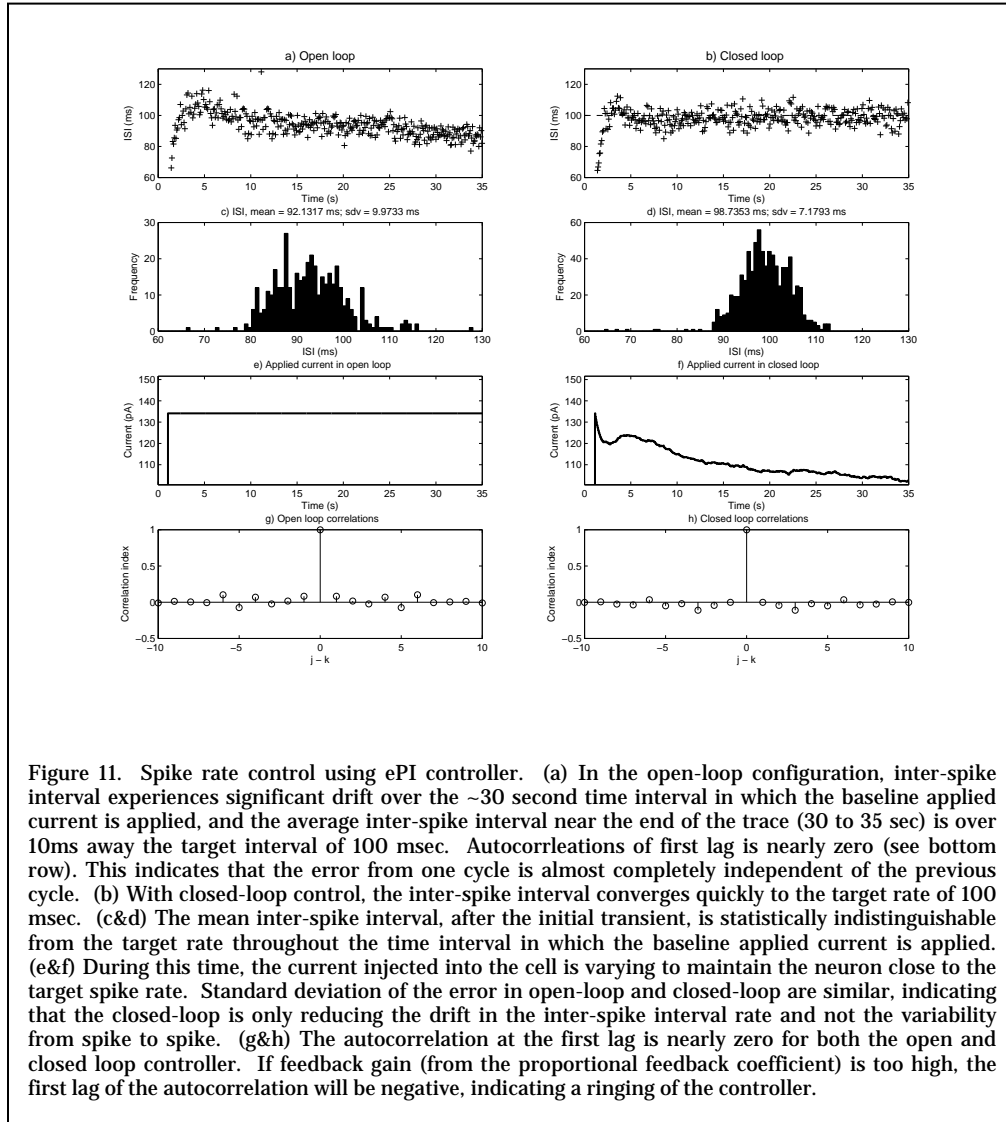


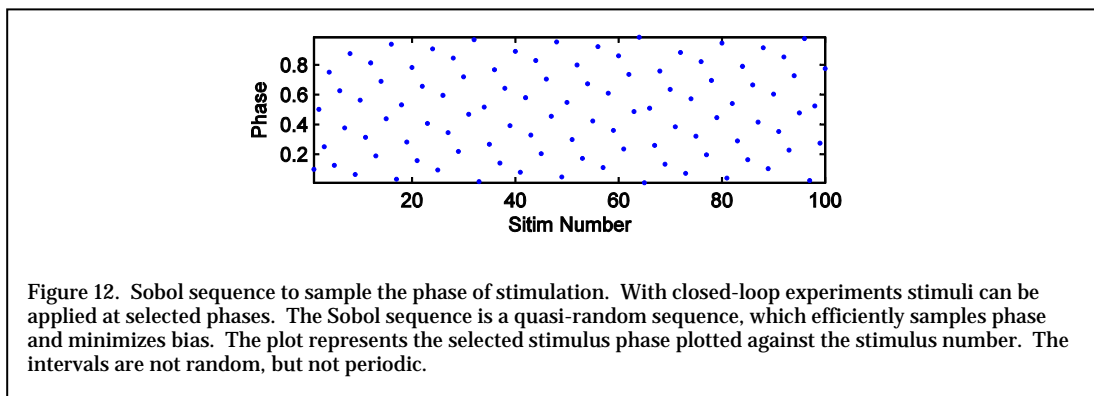
Figure 11. Spike rate control using ePI controller. (a) In the open-loop configuration, inter-spike interval experiences significant drift over the ~30 second time interval in which the baseline applied current is applied, and the average inter-spike interval near the end of the trace (30 to 35 sec) is over 10ms away the target interval of 100 msec. Autocorrelations of first lag is nearly zero (see bottom row). This indicates that the error from one cycle is almost completely independent of the previous cycle. (b) With closed-loop control, the inter-spike interval converges quickly to the target rate of 100 msec. (c&d) The mean inter-spike interval, after the initial transient, is statistically indistinguishable from the target rate throughout the time interval in which the baseline applied current is applied. (e&f) During this time, the current injected into the cell is varying to maintain the neuron close to the target spike rate. Standard deviation of the error in open-loop and closed-loop are similar, indicating that the closed-loop is only reducing the drift in the inter-spike interval rate and not the variability from spike to spike. (g&h) The autocorrelation at the first lag is nearly zero for both the open and closed loop controller. If feedback gain (from the proportional feedback coefficient) is too high, the first lag of the autocorrelation will be negative, indicating a ringing of the controller.

### 4.3 Phase sampling methods

When generating a PRC for a deterministic computational model of a neuron, it is easy to systematically sample the response to stimuli at various phases by simply stepping through phases of stimulation, while measuring the phase shift in response to each stimulus, and restarting the model neuron at a particular initial condition on the limit cycle after each measurement. In generating PRCs for real neurons, stimuli are delivered sequentially to an oscillating neuron. Experimentally, it is best to leave several unstimulated inter-spike intervals after each stimulus to minimize any interactions between the effects of stimuli. This can be

achieved by periodically stimulating the neuron at intervals several times longer than the neuron's natural period. Assuming that the neuron has some variability in its period (i.e. jitter) or by choosing the ratio between the period of the neuron and the period of stimulation corresponds to an irrational number, this method should sample the period close to uniformly and in an unbiased fashion. The advantage of this somewhat haphazard sampling method is that it can be done open loop. The disadvantage is that, in practice, it may result in oversampling of some phases and undersampling of others.

With a closed-loop experimental system, the phase at which the stimuli are applied can be selected directly (i.e. by triggering the stimuli off of spike times). By randomly selecting the phases of stimulation, you can ensure that there are no biases introduced by the experimental protocol. However, even with randomly selecting phases it does not sample the phases most efficiently. Efficiency is paramount in experiments, because you are racing the slow death of the cell, and thus optimum sampling can improve your PRC estimates. Quasi-random selection of phases, using a "low-discrepancy" sequence such as a Sobol sequence, can cover the phases in  $\frac{1}{\sqrt{N}}$  the time as it would take a random sequence, where  $N$  is the number of data points (Press, 1992). The Sobol sequence as a function of stimulus cycle is illustrated at the bottom of Figure 12.



## 5. Fitting functions to PRCs

The inter-spike intervals measured after applying stimuli can be highly variable for real neurons, even if the stimuli are applied at the same phase. Because of this variability, PRC experiments yield scatter plots of phase shift vs the phase of stimulation. By appropriately fitting noisy PRC data, a functional relationship can be obtained to characterize the mean response of the neuron. This functional form of the PRC can then be used in conjunction with coupled oscillator theory to predict of the network behaviors. In this section, we discuss fitting polynomial functions (section 5.1) and Fourier series to PRC data (section 5.2) and address the issue of determining optimal number of fit coefficients in terms of the Aikake Information Criterion (section 5.3). We also discuss statistical models of the variance in PRC data (section 5.4).

### 5.1 Polynomials

Simple functions that are sufficiently flexible to accommodate the shapes of PRCs are polynomials (Netoff et al., 2005; Tateno & Robinson, 2007). Fitting polynomials to PRC data is easy to implement: Matlab and many other data analysis programs have built-in functions that provide the coefficients of a  $k^{\text{th}}$  degree polynomial to fit data in the least squares sense. A  $k^{\text{th}}$  order polynomial fit to PRC data has the form

$$PRC(\phi) = C_k\phi^k + C_{k-1}\phi^{k-1} + \dots + C_2\phi^2 + C_1\phi + C_0,$$

where  $PRC(\phi)$  is the change in phase as a function of the phase of the stimulus  $\phi$ ,  $C_x$ 's are the coefficients that are determined by the fit to the data.

Often, spiking neurons are insensitive to perturbations during and immediately following spikes. This property is manifested in PRCs with noisy but flat portions at the early phases, which can sometimes cause spurious oscillations in polynomial fits. These oscillations in the fit

can be reduced or eliminated by constraining the PRC to be zero at  $\phi = 0$  by using the following constrained polynomial:

$$PRC(\phi) = (C_k\phi^k + \dots + C_2\phi^2 + C_1\phi + C_0) \phi$$

Moreover, because excitatory inputs can only advance the phase of the next spike to the point that the neuron actually spikes, excitatory synaptic inputs to spiking neurons generally elicit a PRC with no phase shifts at  $\phi = 1$ . Thus, it is useful to constrain the fit of the PRC to be zero at both  $\phi = 0$  and  $\phi = 1$ ,

$$PRC(\phi) = (C_k\phi^k + \dots + C_2\phi^2 + C_1\phi + C_0)\phi(1 - \phi).$$

To obtain a constrained polynomial for the general period-1 polynomial case, a constant term  $C_*$  must be added to the above polynomial (Tateno & Robinson, 2007).

Examples of a two-end constrained fit and a no-constraint fit to raw PRC data generated with excitatory stimuli are illustrated in Figure 13. Figure 14 shows examples of a one-end constrained fit ( $PRC(\phi) = 0$ ), a two-end constrained fit and a no-constraint fit for PRC data generated with inhibitory inputs. In the case of inhibitory input, there are almost zero phase shifts at early phases, but input causes considerable phase shifts at late phases.

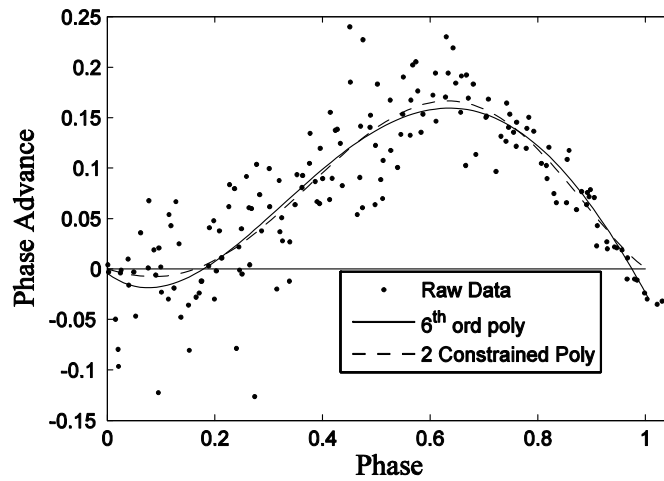


Figure 13. Free and constrained polynomial fits to PRC data for excitatory input to a neuron. Phase advance as a function of stimulus phase is measured for a pyramidal neuron in hippocampus. The neuron was firing at 10 Hz (100 msec intervals). The solid line is an unconstrained 6<sup>th</sup> order polynomial fit (using 7 coefficients) to the points. Notice that the line does not meet the (0,0) point or the (1,0). The dashed line is a two-ended constrained polynomial fit (4 coefficients and 2 constraints) that forces the curve to start at (0,0) and end at (1,0).

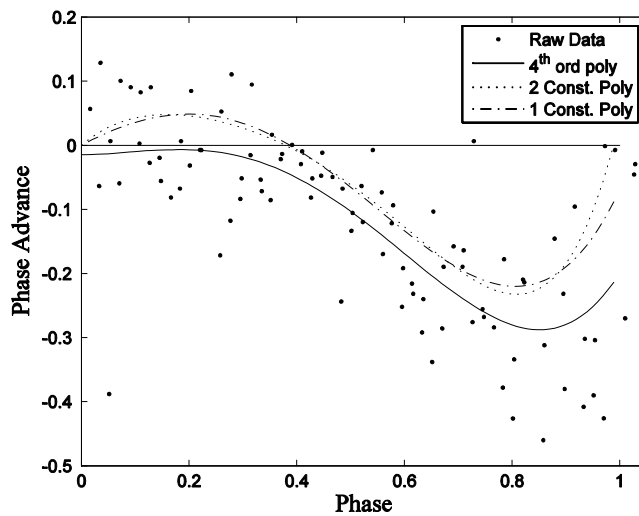


Figure 14. Fits to PRC data generated with inhibitory input. PRCs generated with inhibitory inputs have different shapes than those generated with excitatory curves. This is predominantly because phase shifts are not limited by causality. The largest delays usually occur immediately prior to the neuron spiking. A 4<sup>th</sup> order polynomial (5 coefficients) fit is plotted with a solid line. A 6<sup>th</sup> order polynomial fit (4 coefficients and 2 constraints) with the beginning constrained to (0,0) and the end to (1,0) is plotted with a dotted line. This function does not fit the right hand side of the data well. A 5<sup>th</sup> order polynomial fit (4 coefficients and 1 constraint) constrained only at the beginning to (0,0) is plotted with a dot-dashed line. This curve provides the best fit to the data.

## 5.2 Fourier series

Due to the periodic nature of many PRCs, PRC data is often fit using Fourier series (e.g. Galan, Ermentrout, & Urban, 2005; Mancilla, Lewis, Pinto, Rinzel, & Connors, 2007; K. Ota, Nomura, & Aoyagi, 2009). A  $k^{\text{th}}$  order Fourier series fit to PRC data can be written as

$$PRC(\phi) = a_0 + \sum_{j=1}^k \{a_j \cos(2\pi j\phi) + b_j \sin(2\pi j\phi)\},$$

where the Fourier coefficients are given by

$$a_0 = \frac{1}{N} \sum_{n=1}^N \Delta\phi_n, \quad a_j = \frac{2}{N} \sum_{n=1}^N \Delta\phi_n \cos(2\pi j\phi_n), \quad b_j = \frac{2}{N} \sum_{n=1}^N \Delta\phi_n \sin(2\pi j\phi_n),$$

where  $\Delta\phi_n$  is the phase advance measured on stimulus number  $n$  that was delivered at phase  $\phi_n$ , and  $N$  is the number of data samples. Because many PRCs are zero for  $\phi = 0$  and  $\phi = 1$ , a better fit for fewer parameters can sometimes be obtained by using the Fourier sine series

$$PRC(\phi) = \sum_{j=1}^k b_j \sin(\pi j\phi), \quad b_j = \frac{2}{N} \sum_{n=1}^N \Delta\phi_n \sin(\pi j\phi_n).$$

Figure 15 illustrates PRC data that is fit using the Fourier sine series with  $k = 1, 2, 3$  and 10. It can be seen that the PRC data set is fit well with only the first few modes. Seemingly spurious oscillations appear when the first 10 modes are used to fit the PRC data, suggesting the data are over fit.

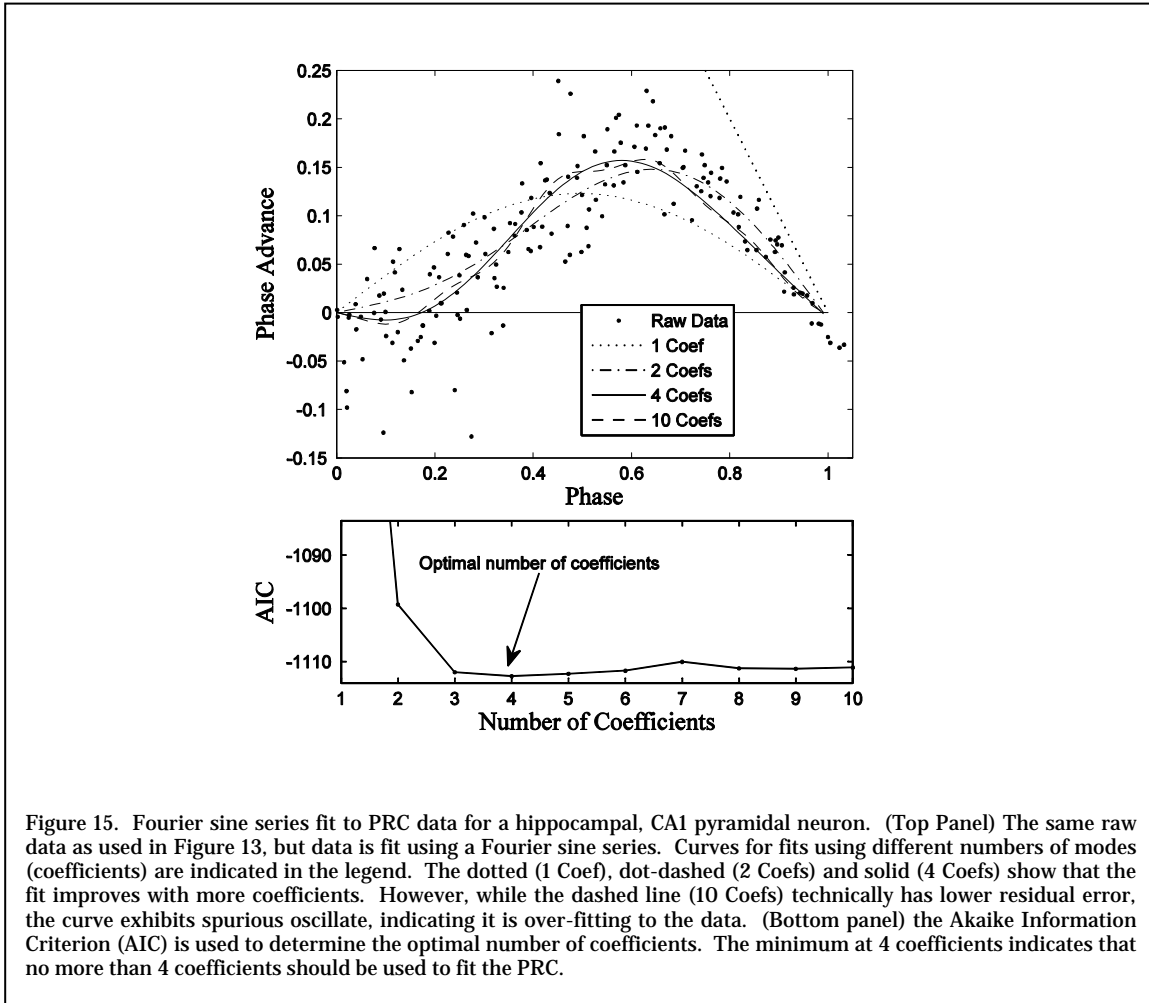


Figure 15. Fourier sine series fit to PRC data for a hippocampal, CA1 pyramidal neuron. (Top Panel) The same raw data as used in Figure 13, but data is fit using a Fourier sine series. Curves for fits using different numbers of modes (coefficients) are indicated in the legend. The dotted (1 Coef), dot-dashed (2 Coefs) and solid (4 Coefs) show that the fit improves with more coefficients. However, while the dashed line (10 Coefs) technically has lower residual error, the curve exhibits spurious oscillate, indicating it is over-fitting to the data. (Bottom panel) the Akaike Information Criterion (AIC) is used to determine the optimal number of coefficients. The minimum at 4 coefficients indicates that no more than 4 coefficients should be used to fit the PRC.

One advantage that Fourier series has over polynomials is that one can get a reasonably good idea of the shape of the PRC by considering the values of the coefficients. Furthermore, the  $H$ -function, which is defined as  $H(\Delta_i) = \Delta_{i+1} - \Delta_i \approx PRC_1(\Delta_i) + PRC_2(1 - \Delta_i)$ , where  $PRC_1(\Delta_i)$  represents the phase advance of cell 1 given the synaptic input from cell 2 and  $PRC_2(1 - \Delta_i)$  is phase advance of cell 2 given the approximate phase of cell 1's input (assuming the phase advance of cell 1 from cell 2's input is nearly zero). This is the difference between the two neuron's spikes on can simply be estimated by summing only the odd Fourier Coefficients (Galán, Ermentrout, & Urban, 2006).

### 5.3 Over- and under-fitting PRC data: Akaike information criterion (AIC)

Because Fourier modes are orthogonal to one another, each Fourier Coefficient can be determined sequentially<sup>5</sup> and the fitting process can be stopped when the quality of the fit is satisfactory. As indicated above, when too few modes are included, the data will not be well fit, and as more modes are included, the residual error of the fit will decrease. However, while including additional modes can decrease the residual error, the decreased error may not be justified by the additional fitting parameters. To determine how many modes (i.e. number of fitting parameters) should be included, one can use the Akaike information criterion (AIC) (Burnham & Anderson, 1998). The Akaike information criterion<sup>6</sup> is calculated using the function

$$AIC(k) = 2k + n \left( \ln \left( \frac{1}{n} \sum_{j=1}^n \epsilon_j(k)^2 \right) \right)$$

where  $k$  is the number of fitting parameters (e.g. Fourier coefficients),  $n$  is the number of points in the data set, and  $\epsilon_j(k)$  is the residual error for the  $j^{\text{th}}$  data point to the fitted PRC using the  $k$  fitting parameters. The optimal number of parameters is determined when  $AIC(k)$  is at its minimum. In Figure 15 (bottom),  $AIC$  is plotted as a function of the number of parameters used to fit neuronal PRC data. It can be seen that the minimum occurs at  $k = 4$ , thus using more than 4 Fourier modes is over-fitting the PRC data.

The AIC can be used in a similar manner to select the optimal number of coefficients for polynomial fits. In fact, the AIC can be used to determine which model (i.e. a Fourier series, a constrained polynomial, etc.) yields the optimal fit. We note however that the AIC does not determine whether the fits are statistically significant.

---

<sup>5</sup> Note that this could be done for polynomial fits too by using orthogonal polynomials (e.g. Legendre or Chebychev polynomials).

<sup>6</sup> This formula for the  $AIC$  assumes that errors are independently distributed and described by a Gaussian distribution.

There are alternative approaches to check for validity of fits to PRC data. Galan et al. (2005) fit raw PRC data with a Fourier series and then tested their fit by comparing it to smoothed data and to fits when the data had been shuffled along the phase axis (abscissa) of the PRC. There are also techniques that employ Bayesian methods to produce a maximum a posteriori (MAP) estimation of the iPRC ((K. Ota, Omori, & Aonishi, 2009) see also Chapter Q).

#### **5.4 Fitting noise around the PRC**

PRC data for real neurons can be quite noisy. Models that use PRCs to predict phase-locking dynamics usually do not account for the variable phase-response properties of neurons. Accounting for the variance of PRC data into these models could provide insight into inherently stochastic behaviors such as random leader swapping and jitter around 'stable' phase-locked states. Therefore, it could be very useful to obtain a good description of the variability of PRC data.

The variance in PRC data could be generated from several sources. One source of variability could be due to external synaptic noise, which will influence the neurons' spike times along with the simulated input applied through the electrode. We find that blocking synaptic inputs in slice experiments did not dramatically reduce the variability (Netoff, unpublished), indicating that synaptic noise may not be a major source of variability of *in vitro* PRC data. Another source of variability could be the stochastic fluctuation of the ion channels in the neurons themselves. It has not yet been identified how much of the variability can be attributed to this source. Identifying the source of the noise may be important in determining how the variability is related to the shape of the PRC, i.e. the variability in spike time may be phase dependent.

The variance around the PRC can be strongly phase dependent, as can be seen in Figure 13 and Figure 16. For moderate to large sized inputs, the variability in response to excitatory inputs earlier in the cycle is usually greater than inputs arriving at the end of the cycle. There are two causes for the decreased variability at late phases. One is that, as the neuron approaches

threshold towards the end of the cycle, synaptic inputs are more likely to directly elicit an action potential. A directly elicited action potential has significantly less variability than a spike whose time has been modulated by synaptic inputs early in the cycle. Inhibitory synaptic inputs generally do not elicit an action potential, and therefore generate PRCs with more uniform variability across phase, as shown in Figure 14.

The simplest way to estimate the noise is to bin the data and estimate the standard deviation in each phase bin. The drawback to this method is that dividing the data into finer temporal bins results in fewer points in each bin and a less accurate estimate of the standard deviation. This also leads to a piecewise model of the variance.

Another approach is to fit a continuous function relating the variance to the phase. A simple function that can be fit to the standard deviation around the PRC data for excitatory stimuli is  $\hat{\sigma}(\phi) = n_1 + n_2\sqrt{1 - \phi}$ . At the end of the cycle when  $\phi = 1$ , the second term is zero and the standard deviation is equal to  $n_1$ . As the phase of the input decreases, the variance increases as a square root of the phase. The motivation for this function is ad-hoc, but is based on the premise that the noise is summed from the time of the synaptic input to the end of the period. Therefore, the variance increases linearly in time (and the standard deviation as a square root) as the synaptic input is applied earlier in the phase.

Fitting a function to the noise is not as easy as fitting a function to the mean. Rather than optimizing the least squares error from the fit function, we must find the maximum likelihood function instead. First, we start with the removing our best estimate of the PRC from the raw data  $r(i) = DATA\_PRC(\phi(i)) - PRC\_FIT(\phi(i))$  to get the residuals. The residuals of the PRC are plotted in lower panel of Figure 16. Next, we need to estimate the probability of seeing the actual measured inter-spike intervals given an estimate of the variance at each phase. We can choose the initial conditions for the function  $\hat{\sigma}(\phi)$  as:  $n_1 = \sqrt{\frac{1}{n} \sum_i^n r(i)^2}$  and slope  $n_2 = 0$ . Assuming that the residuals are Gaussianly distributed and independent, the probability of

observing each point given our function for the variance is  $p(i) = \frac{1}{\hat{\sigma}(i)\sqrt{2\pi}} \exp\left(-\frac{r(i)^2}{2\hat{\sigma}(i)^2}\right)$ . The total likelihood of all the points observed is the product of the probabilities at each point,  $\mathcal{L} = \prod_i^n p(i)$ . Because this probability can become very small very quickly and approach the limits of the machine precision, it is usually calculated as the log-likelihood,  $\log(\mathcal{L}) = -\sum_i^n [\frac{1}{2}\log(2\pi\hat{\sigma}(i)^2) + \log(p(i))]$ . Optimizing the log-likelihood by adjusting the parameters of  $\hat{\sigma}$ , we can fit the function to the variance of the data. Standard deviation as a function of phase fitting our function to the noise is shown in Figure 16.

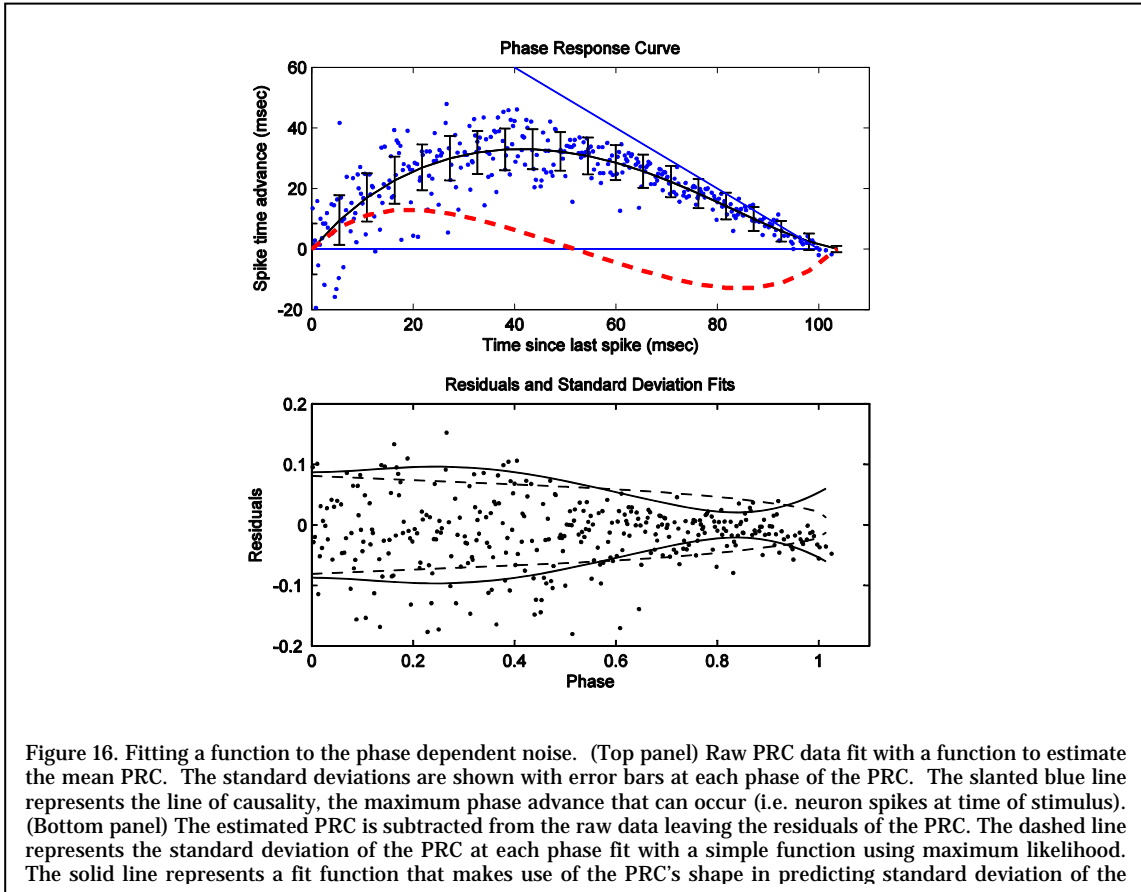
Recently, Ermentrout, Beverlin & Netoff (submitted) has shown that, when a neuron is subjected to additive white noise, the relationship between the variance in phase response of a neuron and the shape of the iPRC ( $Z$ ) is

$$\text{var}(\phi) = \epsilon^2 \left( [1 + \beta Z'(\phi)]^2 \int_0^\phi Z^2(s) ds + \int_\phi^T Z^2(s + \beta Z(\phi)) ds \right),$$

where  $\epsilon$  is the magnitude of the (white) noise and  $\beta$  is the strength of the (delta-function) stimulus. Note that, to leading order in  $\beta$ , this variance is phase independent for small  $\beta$  and is equivalent to the intrinsic jitter in the ISIs

$$\text{var}(\phi) = \epsilon^2 \left( \int_0^T Z^2(s) ds \right).$$

The parameters  $\epsilon$  and  $\beta$  are usually unknown, therefore are used as free parameters to fit the function to the data optimizing the maximum likelihood. Fits to the residuals using this function is plotted in Figure 16. This function gives slightly higher accuracy in fitting the variance over the simpler square-root function given the same number of free parameters.



## 6. Measuring iPRC with "White Noise" Stimuli

In this section, we outline an alternative method for measuring the infinitesimal phase response curve (iPRC). The method consists of continuously stimulating the neuron with a small-amplitude highly-fluctuating input over many inter-spike intervals, measuring the phase shifts of all spikes due to the stimulus, and then deconvolving the stimulus and the phase-shifts to obtain the iPRC. The method is suggested in Izhikevich (Izhikevich, 2007) and is related to work in Ermentrout et al. (Ermentrout, Galan, & Urban, 2007) and Ota et al. (K. Ota et al., 2009).

As described in section 2.3, we assume that the stimuli are sufficiently small so that stimulus has a linear effect on the phase of the neuron. Therefore, the phase shift  $\Delta\psi_k$  of the  $k^{\text{th}}$

spike during the stimulus is approximated by integral of the product of the iPRC  $Z(t)$  and the stimulus  $I_{stim,k}(t) = \sigma \xi_k(t)$  over the  $k^{\text{th}}$  inter-spike interval

$$\Delta\psi_k = T - T_k \cong \int_0^{T_k} Z(\theta(t)) \sigma \xi_k(t) dt \quad (12)$$

where  $T_k$  is the duration of the  $k^{\text{th}}$  inter-spike interval,  $T$  is the intrinsic period of the neuron, and  $\theta(t)$  is the absolute phase of the neuron. The stimulus  $\sigma \xi_k(t)$  is chosen to be a piecewise constant function that is a realization of Gaussian white noise, i.e. time is broken up into very small intervals of width  $\Delta t$  and the amplitudes of  $\sigma \xi_k(t)$  in each subinterval is drawn from a Gaussian distribution with zero mean and variance  $\sigma^2$ , where  $\sigma$  is assumed to be small. Note that this stimulus is composed of a wide range of Fourier modes that will typically form a basis for the iPRC  $Z$ .

The phase of the unstimulated neuron increases linearly with time, and therefore we approximate the phase of the weakly stimulated neuron as  $\theta(t) = T/T_k t$ . By changing variables so that the integration is in terms of phase, equation 12 becomes

$$\Delta\psi_k \cong \int_{\theta=0}^T Z(\theta) \sigma \xi_k(t(\theta)) \frac{T_k}{T} d\theta \quad (13)$$

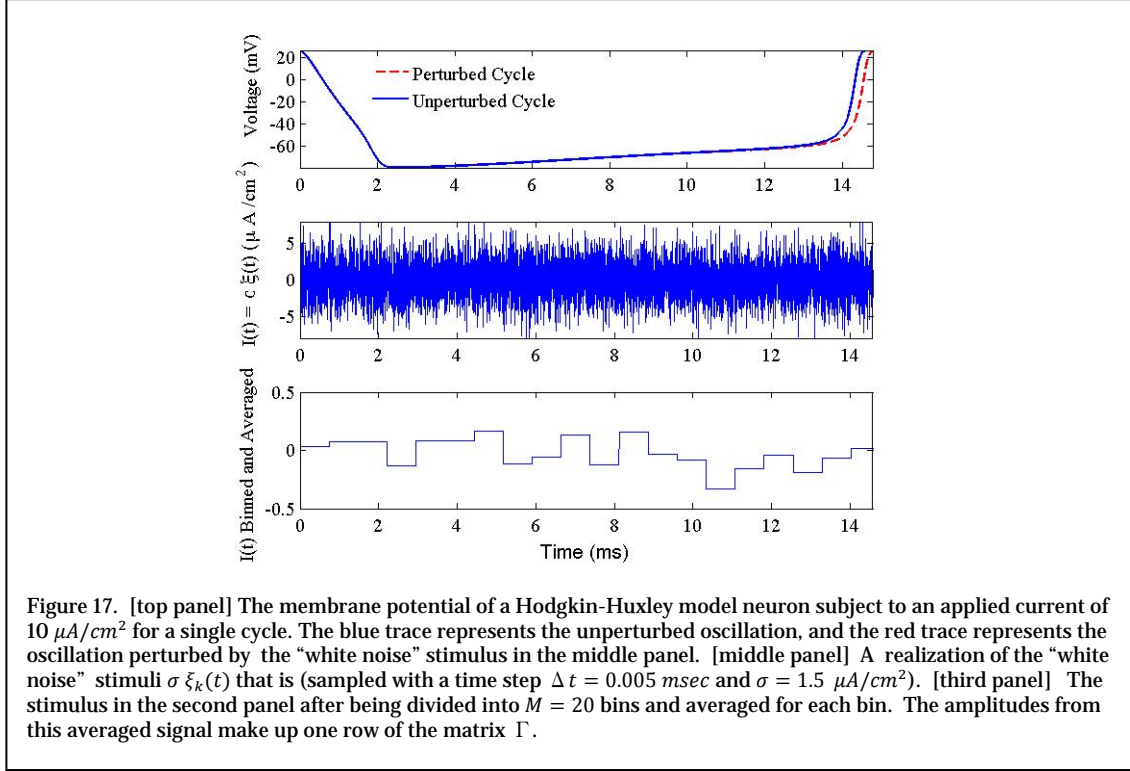
Note that, in this form, the upper limit of integration is independent of  $k$ , i.e. it is the same for all cycles. By discretizing phase into  $M \sim 20$  equal bins of width  $\Delta\theta = T/M$ , equation 13 can be approximated using a middle Riemann sum

$$\Delta\psi_k \cong \sum_{j=1}^M Z(\theta_j) \langle \sigma \xi_k(t_j) \rangle \frac{T_k}{T} \Delta\theta \quad (14)$$

where  $\langle \sigma \xi_k(t_j) \rangle$  is the average of the stimulus in the  $j^{\text{th}}$  bin during the  $k^{\text{th}}$  cycle

$$\langle \sigma \xi_k(t_j) \rangle = \frac{1}{\Delta} \int_{t_j - \Delta/2}^{t_j + \Delta/2} \sigma \xi_k(t) dt.$$

and  $\theta_j = \left(j - \frac{1}{2}\right) \Delta\theta$ ,  $t_j = \frac{T_k}{T} \theta_j$ , and  $\Delta_k = \frac{T_k}{T} \Delta\theta$ . Figure 17 shows an example of a fluctuating stimuli (second panel) and its binned and averaged version for a single cycle and  $M = 20$ .

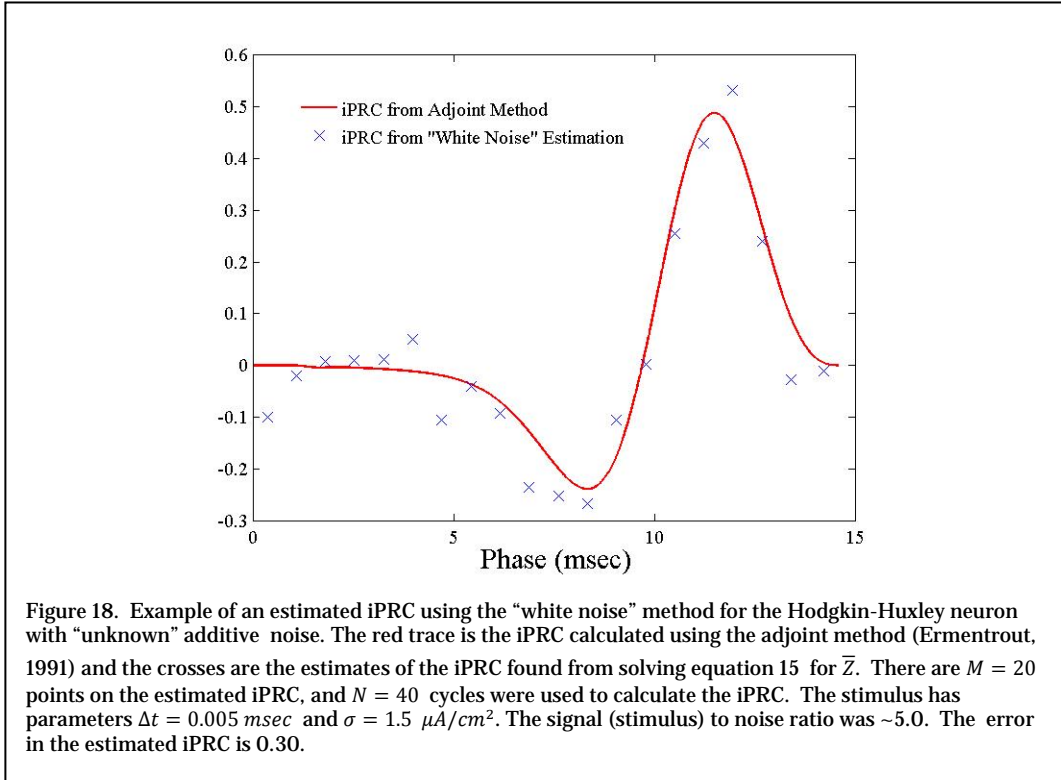


If the stimulus is presented over  $N$  cycles, equation 14 with  $k = 1 \dots N$  yields a system of  $N$  equations with  $M$  unknowns, i.e. the equally spaced points on the iPRC  $Z(\theta_j)$ . In matrix notation, this system of equations is

$$\overline{\Delta\psi} \cong \Gamma \bar{Z} \quad (15)$$

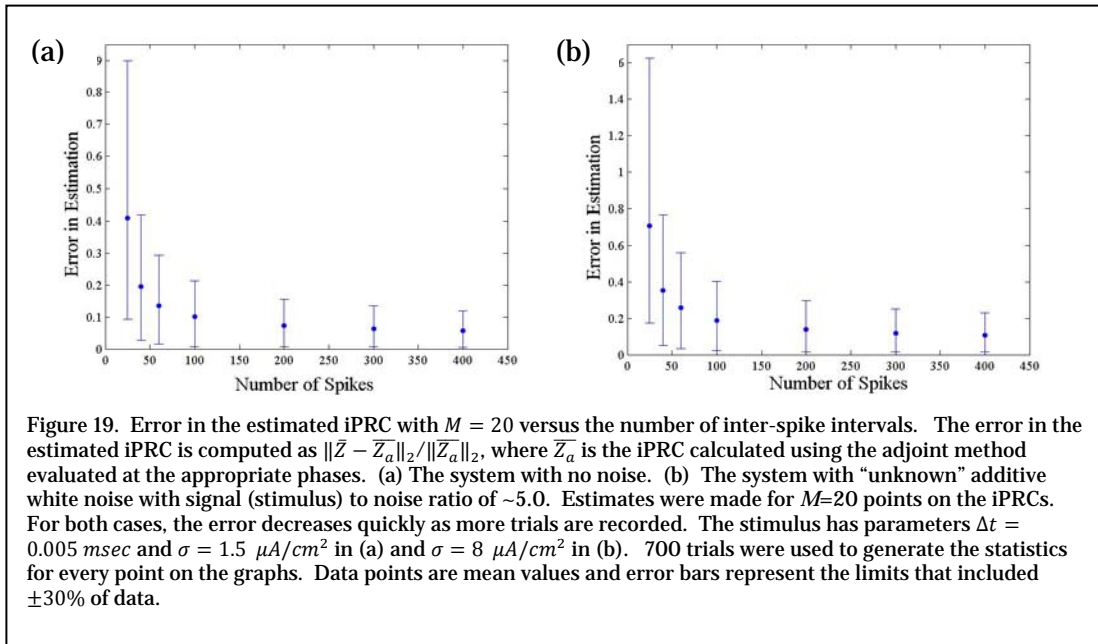
where  $\overline{\Delta\psi}$  is an  $N \times 1$  vector containing the phase shifts of each spike during the stimulus,  $\Gamma$  is an  $N \times M$  matrix in which the  $j,k$  element is  $\langle \sigma \xi_k(t_j) \rangle \frac{T_k}{T} \Delta\theta$  containing the binned and averaged stimuli for each spike, and  $\bar{Z}$  is a  $M \times 1$  vector containing the points on the iPRC. Thus, estimation of the iPRC is reduced to solving a ‘simple’ linear algebra problem. Typically, there should be more phase shifts recorded ( $N$ ) than points on the iPRC ( $M$ ), so that system equation 15 is over-determined and can be solved using a least squares approximation. Figure 18 shows

an example of an iPRC estimated using this technique for the Hodgkin-Huxley (HH) model neuron with additive current noise. There are 20 points on the estimated iPRC ( $M = 20$ ) and 40 spikes were sampled ( $N = 40$ ). The error in this estimated iPRC is 0.30, where the error is computed as the normalized  $\ell_2$ -norm  $\|\bar{Z} - \bar{Z}_a\|_2 / \|\bar{Z}_a\|_2$ , where  $\bar{Z}_a$  is the iPRC calculated using the adjoint method evaluated at the appropriate phases.

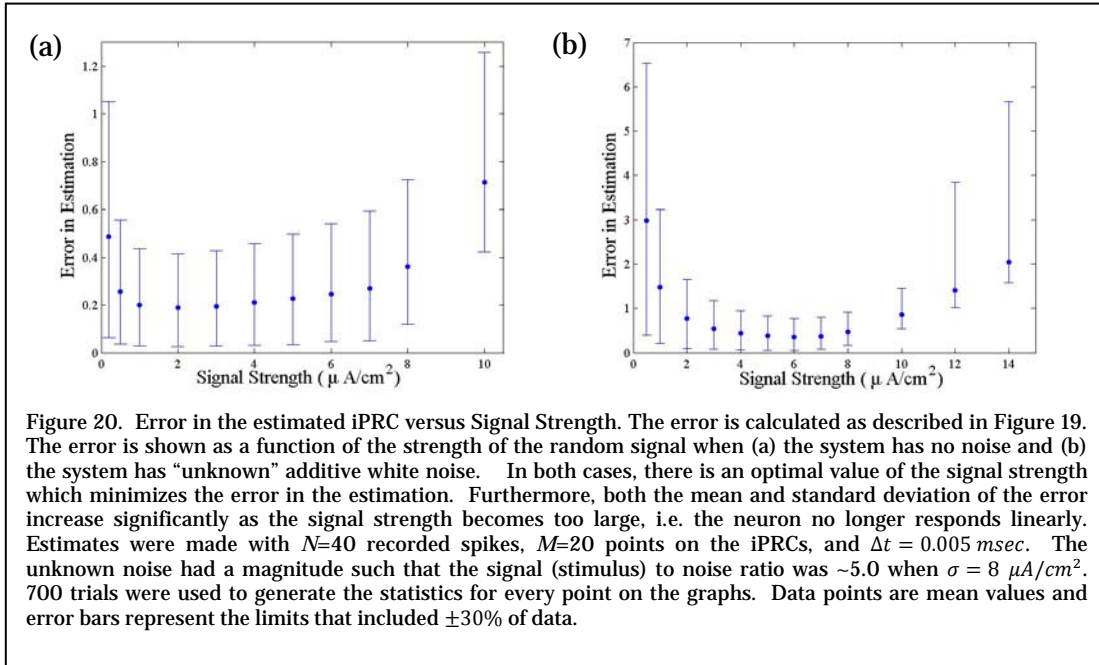


Because  $\Gamma$  is a random matrix, it could sometimes have a high condition number, which could lead to significant error in the estimation of the discretized iPRC  $\bar{Z}$ . However, we can reduce the chance of this error by making the number of spikes considered  $N$  sufficiently larger than the number of points on the estimated iPRC  $M$ . Figure 19 shows the decrease in the error of the estimation of the iPRC for the HH model neuron as the number of spikes is increased. Note the steep initial decrease in the error. In practice, we find that about twice as many spikes (phase shifts) as number of points on the estimated iPRC yields a relatively low error. Typically, 20 points provides a good representation of an iPRC for a spiking neuron. Therefore, if a

neuron is firing at 10-20 *Hz* on average, and the phase shifts are measured over 40 spikes, it only takes 2-4 seconds to record the data needed to estimate the iPRC.



The strength of the random stimulus,  $\sigma$ , also affects the quality of the estimated iPRC. In practice, the stimulus amplitude must be small in order for the estimation to be theoretically valid, but it must also be large enough to overcome the intrinsic noise in the system. Figure 20 plots the error in the estimation as a function of  $\sigma$  when there is no unknown additive noise in the system (a), and when there is unknown additive noise in the system (b). In both cases, there is an optimal value of  $\sigma$  that minimizes the error in our estimation. This optimal value is larger when there is noise in the system.



While the method described above is perhaps the most straightforward “white noise” method, other methods that use white noise stimuli to measure the iPRC have also been proposed. Ermentrout et al. 2007 showed that, when an oscillating neuron is stimulated with small amplitude white noise, the spike triggered average (STA) is proportional to the derivative of its iPRC. As such, the iPRC can be calculated by integrating the STA. Ota (K. Ota et al., 2009) recently addressed several practical issues concerning the results of Ermentrout (Ermentrout et al., 2007) and outlined a procedure to estimate iPRCs for real neurons by using an appropriately weighted STA.

Izhikevich (Izhikevich, 2007) comments that white noise methods for iPRC estimation should be more immune to noise than standard pulse methods because the stimulus fluctuations are spread over the entire cycle and not concentrated at the moments of pulses. However, to our knowledge, there has been no systematic comparison of the white noise methods and the standard pulse method. More work is needed to determine the optimal method for different situations (i.e. different noise levels, limitations on number of spikes, etc.). Furthermore, we expect that refinements could be made to improve most of these methods.

## Summary

- The first step in generating a phase response curve for a neuron is choosing an appropriate stimulus waveform. When estimating the infinitesimal PRC (for use with theory of weakly coupled oscillators), a small brief delta-function-like stimulus pulse can be used. If synaptic inputs are not expected to sum linearly, then a realistic synaptic waveform should be used to measure the PRC to include the proper nonlinear responses of the neuron.
- The effects of a pulse stimulus on neuronal firing may last longer than a single cycle and give rise to measureable changes in ISIs in the cycles following the stimulated interval. These effects can be quantified with secondary and higher order PRCs and can be incorporated into models to increase their accuracy (Maran & Canavier, 2008; Oprisan & Canavier, 2001). Alternatively, the stimulus can be repeated at the same phase until the higher order effects accumulate and stabilize, and then the steady state response to the synaptic input at a phase can be measured. This results in measuring a “functional PRC” (Cui et al., 2009).
- Neurons exhibit considerable amounts of noise, making phase response data variable. There are two sources of noise: drift and jitter. Drift in the dynamics of the neuron occurs from slow-time-scale neuronal processes and “run down” (slow death) of the neuron during the experiment. This can be compensated to some degree by maintaining the firing rate of the neuron with a spike rate controller. While it is not a panacea, it keeps one aspect (the period) approximately constant over the duration of the experiment.
- To decrease the duration of the PRC experiment and thereby reduce the effects of drift on PRC estimation, the sampling of stimulus phase can be optimized. Using a Sobol sequence to sample the phases is much more efficient than random, or quasi-periodic sampling.

- The jitter in the phase response can be overcome by fitting a function to the data to estimate the deterministic portion of the neuron's PRC. Polynomials with constraints or Fourier series usually provide good fits to PRC data. The Akaike information criterion can be used to determine the appropriate number of coefficients when fitting either a polynomial or the Fourier series.
- The variability in a neuron's phase response can also be quantified and modeled. Ermentrout, Beverlin & Netoff (submitted) has recently shown that the phase dependence of the variance is dependent on the shape of the PRC. We also present a simple function that can be fit to the variance by optimizing the maximum likelihood that does a reasonably good job.
- White noise stimulus approaches provide alternatives to pulse stimulation methods for measuring infinitesimal PRCs. This approach uses linear algebra to estimate the iPRC from neuronal response to white noise applied to several periods. More work must be done to optimize these methods and to systematically compare them to the standard pulse stimulation methods.

*Acknowledgements:* TJJ and MAS were supported by the National Science Foundation under grants DMS-09211039 (TJJ), DMS-0518022 (TJJ), TIN was supported by NSF CAREER Award CBET-0954797 (TIN).

## References

### References

- Burnham, K. P., & Anderson, D. R. (1998). *Model selection and inference : A practical information-theoretic approach*. New York: Springer.
- Canavier, C. C. (2005). The application of phase resetting curves to the analysis of pattern generating circuits containing bursting neurons. In S. Coombes, P. C. Bressloff & N. J. Hackensack (Eds.), *Bursting: The genesis of rhythm in the nervous system* (pp. 175-200) World Scientific Pub.
- Cruikshank, S. J., Lewis, T. J., & Connors, B. W. (2007). Synaptic basis for intense thalamocortical activation of feedforward inhibitory cells in neocortex. *Nature Neuroscience*, *10*(4), 462-468. doi:10.1038/nn1861
- Cui, J., Canavier, C. C., & Butera, R. J. (2009). Functional phase response curves: A method for understanding synchronization of adapting neurons. *Journal of Neurophysiology*, *102*(1), 387-398. doi:10.1152/jn.00037.2009
- Dorval, A. D., 2nd, Bettencourt, J., Netoff, T. I., & White, J. A. (2007). Hybrid neuronal network studies under dynamic clamp. *Methods in Molecular Biology (Clifton, N.J.)*, *403*, 219-231. doi:10.1007/978-1-59745-529-9\_15
- Dorval, A. D., Bettencourt, J. C., Netoff, T. I., & White, J. A. (2008). Hybrid neuronal network studies under dynamic clamp. In *Applied patch clamp* () Humana Press.
- Dorval, A. D., Christini, D. J., & White, J. A. (2001). Real-time linux dynamic clamp: A fast and flexible way to construct virtual ion channels in living cells. *Ann Biomed Eng*, *29*(10), 897-907.
- Ermentrout, G. B., & Chow, C. C. (2002). Modeling neural oscillations. *Physiol Behav*, *77*(4-5), 629-633.

- Ermentrout, G. B., Galan, R. F., & Urban, N. N. (2007). Relating neural dynamics to neural coding. *Physical Review Letters*, *99*(24), 248103.
- Ermentrout, G. B., & Kopell, N. (1991). Multiple pulse interactions and averaging in systems of coupled neural oscillators. *J.Math.Biol.*, *29*, 195-217.
- Galan, R. F., Ermentrout, G. B., & Urban, N. N. (2005). Efficient estimation of phase-resetting curves in real neurons and its significance for neural-network modeling. *Physical Review Letters*, *94*(15), 158101.
- Galán, R. F., Bard Ermentrout, G., & Urban, N. N. (2006). Predicting synchronized neural assemblies from experimentally estimated phase-resetting curves. *Neurocomputing*, *69*(10-12), 1112-1115. doi:DOI: 10.1016/j.neucom.2005.12.055
- Golomb, D., & Amitai, Y. (1997). Propagating neuronal discharges in neocortical slices: Computational and experimental study. *Journal of Neurophysiology*, *78*(3), 1199-1211.
- Hille, B. (1992). *Ionic channels of excitable membranes* (2nd ed.). Sunderland, Mass.: Sinauer Associates.
- Izhikevich, E. M. (2007). *Dynamical systems in neuroscience : The geometry of excitability and bursting*. Cambridge, Mass.: MIT Press.
- Kuramoto, Y. (1984). *Chemical oscillations, waves, and turbulence*. Berlin ; New York: Springer-Verlag.
- Lewis, T. J., & Rinzel, J. (2003). Dynamics of spiking neurons connected by both inhibitory and electrical coupling. *Journal of Computational Neuroscience*, *14*(3), 283-309.
- Mancilla, J. G., Lewis, T. J., Pinto, D. J., Rinzel, J., & Connors, B. W. (2007). Synchronization of electrically coupled pairs of inhibitory interneurons in neocortex. *The Journal of Neuroscience : The Official Journal of the Society for Neuroscience*, *27*(8), 2058-2073. doi:10.1523/JNEUROSCI.2715-06.2007

- Maran, S. K., & Canavier, C. C. (2008). Using phase resetting to predict 1:1 and 2:2 locking in two neuron networks in which firing order is not always preserved. *Journal of Computational Neuroscience*, *24*(1), 37-55. doi:10.1007/s10827-007-0040-z
- Miranda-Dominguez, O., Gonía, J., & Netoff, T. I. (2010). Firing rate control of a neuron using a linear proportional-integral controller. *Journal of Neural Engineering*, *7*(6), 066004. doi:10.1088/1741-2560/7/6/066004
- Netoff, T. I., Acker, C. D., Bettencourt, J. C., & White, J. A. (2005). Beyond two-cell networks: Experimental measurement of neuronal responses to multiple synaptic inputs. *Journal of Computational Neuroscience*, *18*(3), 287-295. doi:10.1007/s10827-005-0336-9 [doi]
- Netoff, T. I., Banks, M. I., Dorval, A. D., Acker, C. D., Haas, J. S., Kopell, N., & White, J. A. (2005). Synchronization in hybrid neuronal networks of the hippocampal formation. *Journal of Neurophysiology*, *93*(3), 1197-1208. doi:00982.2004 [pii]; 10.1152/jn.00982.2004 [doi]
- Oprisan, S. A., & Canavier, C. C. (2001). Stability analysis of rings of pulse-coupled oscillators: The effect of phase-resetting in the second cycle after the pulse is important at synchrony and for long pulses. *Differential Equations and Dynamical Systems*, *9*, 243-258.
- Ota, K., Omori, T., & Aonishi, T. (2009). MAP estimation algorithm for phase response curves based on analysis of the observation process. *Journal of Computational Neuroscience*, *26*(2), 185-202. doi:10.1007/s10827-008-0104-8
- Ota, K., Nomura, M., & Aoyagi, T. (2009). Weighted spike-triggered average of a fluctuating stimulus yielding the phase response curve. *Physical Review Letters*, *103*(2), 024101. doi:10.1103/PhysRevLett.103.024101
- Press, W. H. (1992). *Numerical recipes in C : The art of scientific computing* (2nd ed.). Cambridge Cambridgeshire ; New York: Cambridge University Press.
- Prinz, A. A., Abbott, L. F., & Marder, E. (2004). The dynamic clamp comes of age. *Trends in Neurosciences*, *27*(4), 218-224. doi:10.1016/j.tins.2004.02.004

- Sharp, A. A., O'Neil, M. B., Abbott, L. F., & Marder, E. (1993). Dynamic clamp: Computer-generated conductances in real neurons. *J Neurophysiol*, *69*(3), 992-95.
- Tateno, T., & Robinson, H. P. (2007). Phase resetting curves and oscillatory stability in interneurons of rat somatosensory cortex. *Biophysical Journal*, *92*(2), 683-695. doi:10.1529/biophysj.106.088021
- Van Vreeswijk, C., Abbott, L. F., & Ermentrout, G. B. (1994). When inhibition not excitation synchronizes neural firing. *J Comput Neurosci*, *1*(4), 313-21.